(NASA-CR-134628) HIGH-TEMPERATURE, LOW-CYCLE FATIGUE OF ADVANCED COPPER-BASE ALLOYS FOR ROCKET NOZZLES. PART 2: NASA 1.1, (Mar-Test, Inc., Cincinnati, Ohio.) CSCL 11F G3/26

N75-11076

Unclas 53896

NASA CR-134628

HIGH-TEMPERATURE, LOW-CYCLE FATIGUE OF ADVANCED COPPER-BASE ALLOYS FOR ROCKET NOZZLES; PART II - NASA 1.1, GLIDCOP, AND SPUTTERED COPPER ALLOYS.

by: J.B.Conway, R.H.Stentz and J.T.Berling

MAR-TEST INC.

Cincinnati, Ohio

November, 1974

prepared for

NATIONAL AERONAUTICS AND SPACE ADMINISTRATION

NASA Lewis Research Center
Contract NAS3-17777

G.R.Halford, Project Manager

1. Report No.	2. Government Accession No.	3. Recipient's Catalog No.
NASA CR-134628		

4. Title and Subtitle	5. Report Date
High-Temperature, Low-Cycle Fatigue of Advanced Copper-Base Alloys For Rocket Nozzles; Part II - NASA 1.1, Glidcop, and Sputtered Copper Alloys	November, 1974
	6. Performing Organization Code
7. Author(s) J. B. Conway, R. H. Stentz and J. T. Berling	8. Performing Organization Report No. MTI-R004-3-1
	10. Work Unit No.
9. Performing Organization Name and Address Mar-Test Inc. 45 Novner Drive Cincinnati, Ohio 45215	11. Contract or Grant No NAS3-17777
	13. Type of Report and Period Covered Contractor Report March through Sept.1974
12. Sponsoring Agency Name and Address National Aeronautics and Space Administration Lewis Research Center 21000 Brookpark Rd., Cleveland, Ohio 44135	14. Sponsoring Agency Code

15. Supplementary Notes

Project Manager, Dr. G. Halford, NASA-Lewis Research Center
Cleveland, Ohio

16. Abstract

Short-term tensile and low-cycle fatigue data are reported for five advanced copper-base alloys: Sputtered Zr-Cu as- received, sputtered Zr-Cu heat-treated, Glidcop AL-10, and NASA alloys 1-1A and 1-1B. Tensile tests were performed in argon at 538°C using an axial strain rate of 2×10^{-3} sec^{-1}. Yield strength and ultimate tensile strength data are reported along with reduction in area values.
Axial strain controlled low-cycle fatigue tests were performed in argon at 538°C using an axial strain rate of 2×10^{-3} sec^{-1} to define the fatigue life over the range from 100 to 3000 cycles for the five materials studied. It was found that the fatigue characteristics of the NASA 1-1A and NASA 1-1B compositions are essentially identical and represent fatigue life values which are much greater than those for any of the other materials tested. In a more extensive evaluation of the NASA 1-1B alloy the effect of temperature at a strain rate of 2×10^{-3} sec^{-1} was evaluated along with the effect of strain rates of 4×10^{-4} and 1×10^{-2} sec^{-1} at 538°C. Hold-time data are also reported for the NASA 1-1B alloy at 538°C using 5 minute hold periods in tension only and compression only at two different strain range values. Hold periods in tension were shown to be much more detrimental than hold periods in compression.

PRICES SUBJECT TO CHANGE

17. Key Words (Suggested by Author(s))	18. Distribution Statement
Fatigue, Tensile, Hold-Time, Strain Rate, Temperature, Relaxation, Copper-base Alloys	unclassified-unlimited

19. Security Classif. (of this report)	20. Security Classif. (of this page)	21. No. of Pages	22. Price*
unclassified	unclassified		

* For sale by the National Technical Information Service, Springfield, Virginia 22151

NASA-C-168 (Rev. 6-71)

TABLE OF CONTENTS

I - SUMMARY

This report describes the test results obtained in the Task II portion of this program which involved an evaluation of the short-term tensile and low-cycle fatigue behavior of five advanced copper-base alloys. Hourglass-shaped specimens were employed and all tests were performed in high-purity argon (oxygen level below 0.01 percent by volume) using a special environmental test chamber. The materials evaluated were as follows:

NASA 1-1A alloy	(R-21)
NASA 1-1B alloy	(R-22)
Glidcop AL-10 alloy	(R-23)
Sputtered Zr-Cu (as fabricated)	(R-26)
Sputtered Zr-Cu (heat treated)	(R-25)

Duplicate tensile tests were performed for all materials (except for R-26 where only one test was performed) at 538°C using an axial strain rate of 2×10^{-3} sec^{-1}. In addition, the R-22 alloy was selected for a more extensive evaluation and tensile properties were determined at 482° and 593°C using a strain rate of 2×10^{-3} sec^{-1} and at 538°C using strain rates of 4×10^{-4} and 1×10^{-2} sec^{-1}. This testing revealed yield strengths and ultimate tensile strengths at 538°C ranging from about 210 and 225 MN/m^2 respectively for the R-22 alloy to about 66 and 110 MN/m^2 respectively for the R-21 alloy. Reduction in area values ranged from about 98 percent for the R-25 alloy to about 6 percent in the case of the R-23 alloy. At a strain rate of 2×10^{-3} sec^{-1} the yield and ultimate tensile strengths of the R-22 alloy were reduced by about 65 percent as the temperature was increased from 482° to 593°C; reduction in area values decreased slightly between 482° and 538°C. For a test temperature of 538°C an increase in strain rate from 4×10^{-4} to 1×10^{-2} sec^{-1} caused the yield and ultimate tensile strengths of the R-22 alloy to increase by approximately 20 percent. In these tests the reduction in area values increased from about 20 percent to about 55 percent as the strain rate was increased.

A series of low-cycle fatigue tests was performed in argon at 538°C using a strain rate of 2×10^{-3} sec^{-1} to define the fatigue life over the range of 100 to 3000 cycles for the alloys involved (only one test of the R-26 composition). This required a strain range regime from about 5.0 percent to 1.0 percent for the more fatigue resistant materials and a strain range regime between 1.0 and 0.6% for the lower fatigue resistant materials. The two NASA 1-1 alloys exhibited essentially identical fatigue behavior to identify fatigue life values which were much greater than those for any of the other materials evaluated. These data for the NASA 1-1 alloy were found to correspond to a fatigue life that was about twice that exhibited by the

Narloy Z composition studied previously.

A limited study of the effect of temperature on the fatigue life of the NASA 1-1B alloy was performed at strain ranges of 3.0 and 1.2 percent using a strain rate of 2×10^{-3} sec^{-1}. Over the temperature range from 482° to 593°C the fatigue life was constant at a value close to 200 cycles in the higher strain range tests. At the lower strain range, tests were performed only at 593°C and these results were found to be in good agreement with the data at 538°C and suggest a slightly increased fatigue life at the higher temperature.

The effect of strain rate on the fatigue life of the NASA 1-1B alloy was also studied in tests at 538°C. Using strain range values of 3.0 and 1.2 percent a general reduction in the fatigue life was observed as the strain rate was decreased from 2×10^{-3} to 4×10^{-4} sec^{-1}. In addition, a general increase in the fatigue life was observed as the strain rate was increased to 1×10^{-2} sec^{-1}.

A hold period duration of 300 seconds was employed in an evaluation of hold-time effects on the NASA 1-1B composition at 538°C using a strain rate of 2×10^{-3} sec^{-1}. Hold periods in tension were found to be particularly detrimental in that the fatigue life was about an order of magnitude or so below that observed for continuous cycling. The effect was particularly severe at a strain range of 1.2 percent where the hold period in tension reduced the fatigue life from about 2000 cycles to about 85 cycles. Hold periods in compression at a strain range of 3.0 percent appeared to have no detrimental effect on the fatigue life. As a matter of fact the fatigue life seemed to be increased somewhat when the 5 minute compression hold period was introduced. At a strain range of 1.2 percent, however, a very different effect was noted. Hold periods in compression decreased the fatigue life below the continuous cycling results and while the effect was only about one-half that due to the tension hold periods it does represent a reversal of the behavior pattern observed at the higher strain range. Severe dimensional instability was noted at the lower strain range, however, in these compression hold-period tests and for this reason the true hold-time effect might not be indicated by these tests.

II - INTRODUCTION

Regeneratively-cooled, reusable-rocket nozzle liners such as found in the engines of the Space Shuttle, Orbit-to-Orbit Shuttle, Space Tug, etc., undergo a severe thermal strain cycle during each firing. To withstand the severe cycles, the liner material must have a proper combination of high thermal conductivity and high low-cycle fatigue resistance. Copper-base alloys possess these desirable qualities and were thusly chosen for this program. A broad-based NASA-Lewis/MAR-TEST program has been instituted to evaluate several candidate alloys by generating the material property data that are required for the design and life prediction of rocket nozzle liners.

This report deals with the high-temperature tensile and low-cycle fatigue behavior of five advanced copper-base alloys as measured in high purity argon. The materials evaluated in this phase of the program were as follows: NASA 1-1A alloy, NASA 1-1B alloy, Glidcop AL-10, sputtered Zr-Cu (as fabricated), and sputtered Zr-Cu (heat treated). Specimen blank material for the first three alloys was supplied in the form of 2.2 cm diameter rod while the blank material for the other two materials was supplied as 2.2 cm x 1.9 cm x 7.6 cm rectangular sections. These materials were given the code designations: R-21, R-22, R-23, R-26 and R-25 respectively.

The material evaluations specified for this Task II effort were as follows:

1) duplicate tensile tests at 538°C for R-21, R-22, R-23 and R-25 using an axial strain rate of 2×10^{-3} sec^{-1}; one test only of the R-26 material under the above conditions;
2) duplicate tensile tests of the R-22 material at 482° and 593°C using an axial strain rate of 2×10^{-3} sec^{-1};
3) duplicate tensile tests of the R-22 material at 538°C using axial strain rates of 4×10^{-4} and 1×10^{-2} sec^{-1};
4) four axial strain controlled low-cycle fatigue tests of the R-21, R-22, R-23 and R-25 compositions at 538°C using an axial strain rate of 2×10^{-3} sec^{-1} to define the fatigue life in the range from 100 to 3000 cycles; one test only of the R-26 material using a total axial strain range of 2.0 percent;
5) duplicate axial strain controlled low-cycle fatigue tests of the R-22 material at 538°C using strain rates of 4×10^{-4} and 1×10^{-2} sec^{-1} at strain ranges corresponding to cyclic life values of 200 and 2000 cycles as determined in (4) above;
6) duplicate axial strain controlled low-cycle fatigue tests of the R-22 material using a strain rate of 2×10^{-3} sec^{-1} at 482° and 593°C at strain ranges employed in (5) above;

7) duplicate axial strain controlled low-cycle fatigue tests of the R-22 material at 538°C using a strain rate of 2×10^{-3} sec^{-1} at the strain ranges employed in (5) above with a hold period of 300 seconds introduced at peak tensile strain only; similar tests with this same hold period duration introduced at the peak compressive strain point.

All these evaluations were performed in high-purity argon in which the oxygen content was less than 0.01 percent by volume.

As the test program was being performed it was found that the required quantity of R-22 material was not available and, hence, the entire test matrix as planned could not be completed.

All the tensile and fatigue tests were performed using hourglass-shaped specimens. A servo-controlled, hydraulically actuated fatigue testing machine (see NASA CR-134627 for complete description) was used in all these evaluations and the threaded test specimens were mounted in the holding fixtures of the test machine using special threaded adaptors. In order to perform these tests in argon a specially constructed pyrex containment vessel was positioned between the holding fixtures of the fatigue machine and neoprene low-force bellows at either end provided the seal to enable the desired gas purity levels to be maintained throughout the test. Side outlets (with appropriate seals) on this containment vessel provided entrance ports to accommodate the extensometer arms and similar side outlets provided entrance ports for the copper tubing leads to the induction coil. In addition, special ports near the bottom of the containment vessel enabled the thermocouples, used for specimen temperature measurement, to be routed out to the temperature control system. Specimen test temperatures were attained using induction heating and this was provided by positioning a specially designed induction coil around the test specimen (see Figure 1).

All force measurements were made using a load cell mounted within the loading train of the fatigue machine and specimen strains were measured by a specially designed, high temperature diametral extensometer. A special test procedure (see NASA CR-134627) was developed to allow the short-term tensile tests to be performed at a constant strain rate which was maintained throughout the test. In the fatigue tests an analog strain computer was employed which allowed the diametral strain signal to be used in conjunction with the load signal so as to provide an instantaneous value for the axial strain which was then the controlled variable (see NASA CR-134627 for complete description of test procedure).

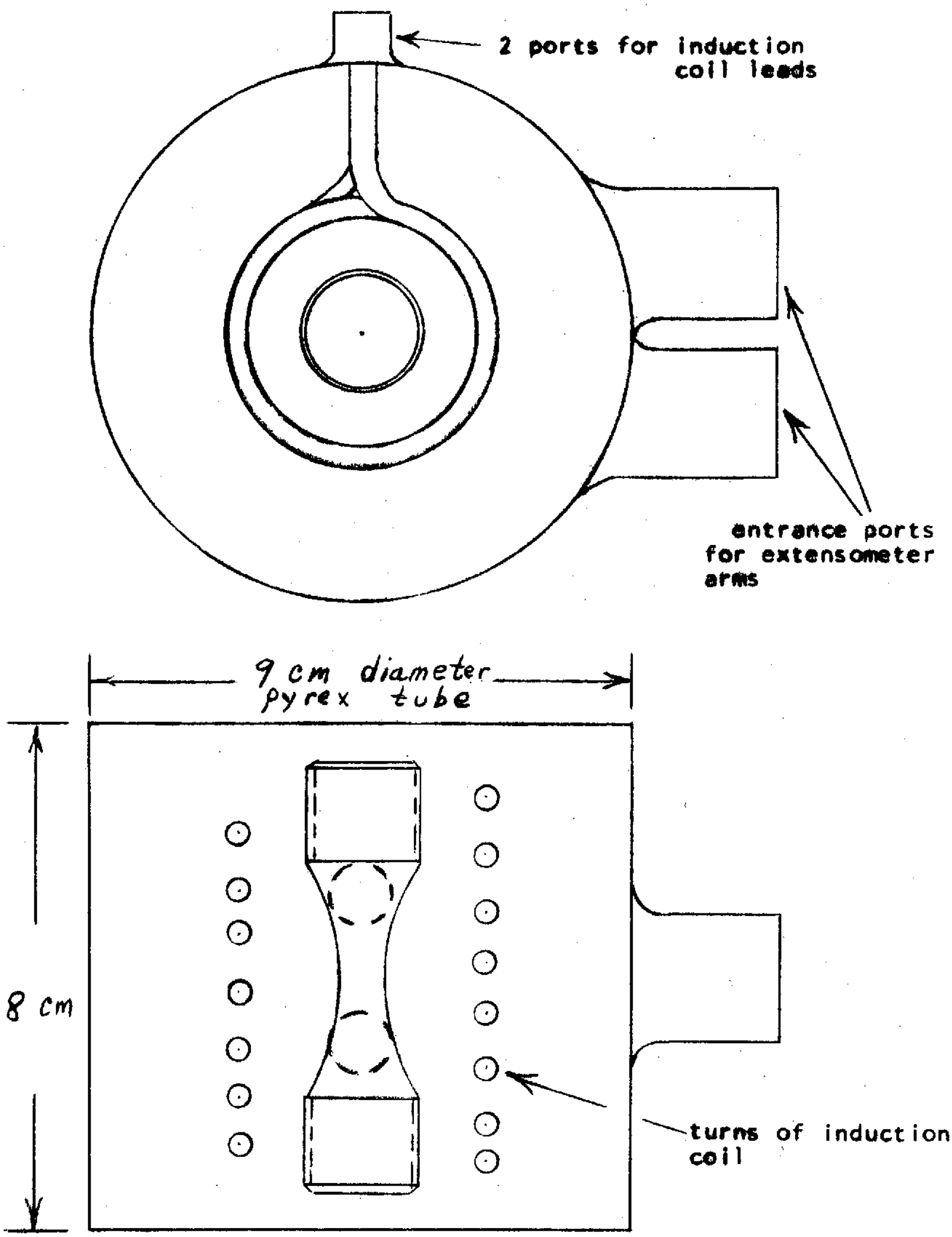

Figure 1- Schematic of Pyrex Environmental Chamber

III - MATERIAL AND SPECIMENS

Specimen material for use in this portion of the program was supplied by NASA-Lewis Research Center, Cleveland, Ohio. A brief description of the five materials evaluated within this task is given in Table I. Specimen blank material for the first three alloys was supplied in the form of 2.2 cm diameter rods while the blank material for the R-25 and R-26 alloys was supplied as 2.2 cm x 1.9 cm rectangular sections about 7.6 cm in length.

Using the specimen design shown in Figure 2 the following specimens were machined:

R-21	8 specimens	(includes 2 spares)
R-22	29 specimens	(includes 2 spares)
R-23	8 specimens	(includes 2 spares)
R-25	8 specimens	(includes 2 spares)
R-26	3 specimens	(includes 1 spare)

It was the original intent to machine 44 specimens of the R-22 alloy in order to accommodate all the different test conditions specified. However after the program was well underway it became clear that the required amount of the R-22 material could not be acquired in time for inclusion in this effort. As a result some of the planned tests could not be performed within this task.

After being machined, all specimens were wrapped in soft tissue paper and placed in individual hard plastic cylinders (about 9 cm in length and 2.2 cm inside diameter). The ends of these cylinders were then sealed with masking tape and the specimen code number was written on the external surface of the cylinder. These cylinders were used for storage before and after test.

In preparing for a test each specimen was subjected to the following:

1) a small longitudinal notch was filed in the threaded sections of the specimen; this was designed to aid in the removal of entrapped air from the threaded area after the specimen was inserted in the adaptors (see below for the specimen-adaptor assembly);
2) the specimen was washed with Freon to remove any surface oils which might have remained after machining;
3) a small quantity of dilute phosphoric acid was applied by hand to the complete surface of the specimen; this removed any surface oxides and any machining oil not removed by the cleaning with Freon; this operation was completed within 15 seconds;
4) the specimen was rinsed in warm water and dried using soft absorbent tissue;
5) the specimen was then subjected to a final cleaning with Freon.

Table 1 - Description of the Materials Evaluated in the Task II Effort

Code No.	Material	Description
R-21	NASA 1-1A	Nominal 1.1% Ag, 0.1% Zr; originally cast as 12.7 cm diameter billet (11.2 kilograms) by AMAX; canned with OFHC sheet and evacuated; heated for hot extrusion to 2.85 cm diameter rods; rods cold reduced to 2.2 cm diameter; aged at 455°C for 4 hours and air cooled
R-22	NASA 1-1B	Same as above except not aged
R-23	Glidcop AL 10 (Trade name of Glidden-Durkee)	0.2% Al_2O_3 copper; as cold reduced to 2.2 cm diameter rods
R-25	Sputtered Zr-Cu; Annealed	Nominal 0.14% Zr-Copper; sputtered; machined into specimen blanks and annealed at 593°C for one hour and air cooled
R-26	Sputtered Zr-Cu; as received	Same as above but not annealed

Figure 2

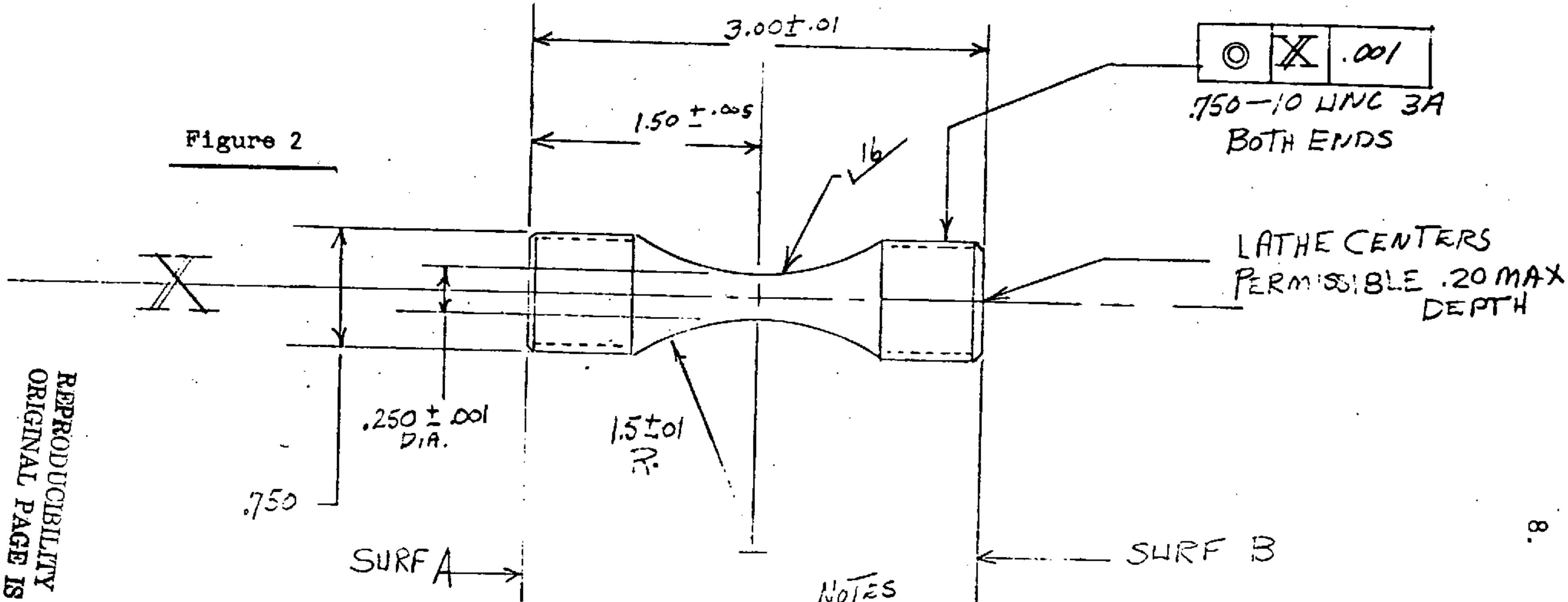

NOTES

1- SURFACES A, & B TO BE PARALLEL WITHIN .001
2- SURFACES A, & B TO BE PERPENDICULAR TO CENTER LINE OF SPECIMEN WITHIN .0005 TIR
3- CONTOURED PORTION OF SPECIMEN TO HAVE A 16 FINISH OR BETTER. FINISHING SHOULD BE IN THE AXIAL DIRECTION USING LOW STRESS LAPPING OR POLISHING OPERATION
~~4- ALL DIA'S TO BE CONCENTRIC WITHIN .001 TI.~~
5- SCREW THREADS TO BE AS LISTED IN NBS HANDBOOK H 28

UNLESS OTHERWISE SPECIFIED DIMENSIONS ARE IN INCHES TOLERANCES ON FRACTIONS ± DECIMALS ± ANGLES ± ALL SURFACES 32	DRAWN DATE APPD ISSUED	SPECIMEN LOW CYCLE FATIGUE
MATERIAL GOVT. OR COML. TO BE SPECIFIED	APPROVED / DATE ENGR 9TC 1-12-71 MFG MATL	Mar-Test inc. CINCINNATI, OHIO
	SCALE 1/1	WT CALC ACTUAL
	SIZE	MTI-1002
	CONT ON SHEET	SH NO.

8

IV. TEST RESULTS AND DISCUSSION OF RESULTS

A) Short-Term Tensile

Short-term tensile tests of the R-21, R-22, R-23 and R-25 materials were performed in duplicate in high-purity argon at 538°C using an axial strain rate of 2×10^{-3} sec^{-1}. In addition, a single test of the R-26 composition was performed at these conditions. A summary of the test results obtained in these short-term tensile evaluations is presented in Table 2. In those tests which were performed in duplicate an excellent reproducibility is noted in the values for yield strength, ultimate strength and reduction in area. Also to be noted are the following:

1) unheat-treated NASA 1-1B alloy (R-22) exhibits much higher yield and tensile strengths than the heat-treated material; the effect of the heat-treatment is also seen in the increase in the reduction in area value from about 32 to 50 percent;
2) the R-23 composition exhibits yield and ultimate strengths which are between the values exhibited by the R-21 and R-22 alloys; however the ductility of the R-23 material at the conditions employed is extremely low;
3) the R-25 and R-26 materials were found to be very ductile at the test conditions employed but were also noted to be very anisotropic; yield and ultimate tensile strengths were close to those exhibited by the R-21 and R-23 materials.

After the tensile data of Table 2 were studied in some detail it was decided to perform a more extensive evaluation of the short-term tensile properties of the R-22 alloy. Tests were performed at 538°C using strain rates of 4×10^{-4} and 1×10^{-2} sec^{-1} and at a temperature of 482° using a strain rate of 2×10^{-3} sec^{-1}. A summary of these test results is presented in Table 3. These results are also presented graphically in Figures 3 and 4 to define the observed temperature and strain rate effects. Because of the limited amount of the R-22 material that was available the tests at 593°C using a strain rate of 2×10^{-3} sec^{-1} were not performed. However, an evaluation of the stress-strain plot during the first loading cycle in the fatigue tests at this temperature and strain rate allowed values for the 0.2% yield strength to be determined. It is these values that are plotted in Figures 3 and 4 to define this property and to establish the trend behavior for the R-22 material (yield strength obtained in this fashion from fatigue tests at 482°C and a strain rate of 2×10^{-3} sec^{-1} were found to be in excellent agreement with the results in Table 3 at these same conditions).

A comparison of some of the short-term tensile results obtained for the R-22 alloy with similar data for the R-24 material (see NASA CR-134627) is presented in Figures 5, 6 and 7. Over the temperature range from 482° to 593°C the yield strength

Table 2 - Short-Term Tensile Properties of Several Copper-Base Alloys Tested in Argon

Diametral Extensometer			Hourglass-Shaped Specimens		
Spec. No.	Temp., °C	Strain Rate, sec^{-1}	0.2% Offset Yield Strength MN/m^2	Ultimate Tensile Strength, MN/m^2	Reduction in Area, %
R-21-1	538	2×10^{-3}	66.0	110.9	51.1
R-21-2	538		68.8	114.4	55.4
R-22-1	538		(a)	220.5	33.4
R-22-2	538		211.3	224.0	32.8
R-22-3	538		209.2	225.1	32.8
R-23-1	538		129.9	147.4	5.5
R-23-2	538		129.2	146.2	6.3
R-23-3	538		122.9	141.1	7.1
R-25-4	538		103.9 (b)	112.8 (b)	97.7 (b)
R-25-5	538		101.1 (b)	102.5 (b)	97.6 (b)
R-26-1	538	2×10^{-3}	77.0 (b)	84.7 (b)	(c)

(a) x-y plot not obtained
(b) approximate value, material very anisotropic
(c) Fracture surface like knife edge, 0.4 cm x 0.1 cm, split and irregular

Table 3 - Short-Term Tensile Properties of NASA 1-1B (R-22) Alloy Tested in Argon

Diametral Extensometer — Hourglass-Shaped Specimens

Spec. No.	Temp. °C	Strain Rate, sec^{-1}	0.2% Offset Yield Strength, MN/m^2	Ultimate Tensile Strength, MN/m^2	Reduction in area, %
R-22-10	482	2×10^{-3}	244.0	252.8	36.0
R-22-15	538	4×10^{-4}	180.8	187.8	20.4
R-22-16	538	4×10^{-4}	180.8	193.4	20.4
R-22-13	538	1×10^{-2}	210.6	223.6	53.8
R-22-14	538	1×10^{-2}	212.4	221.2	56.4

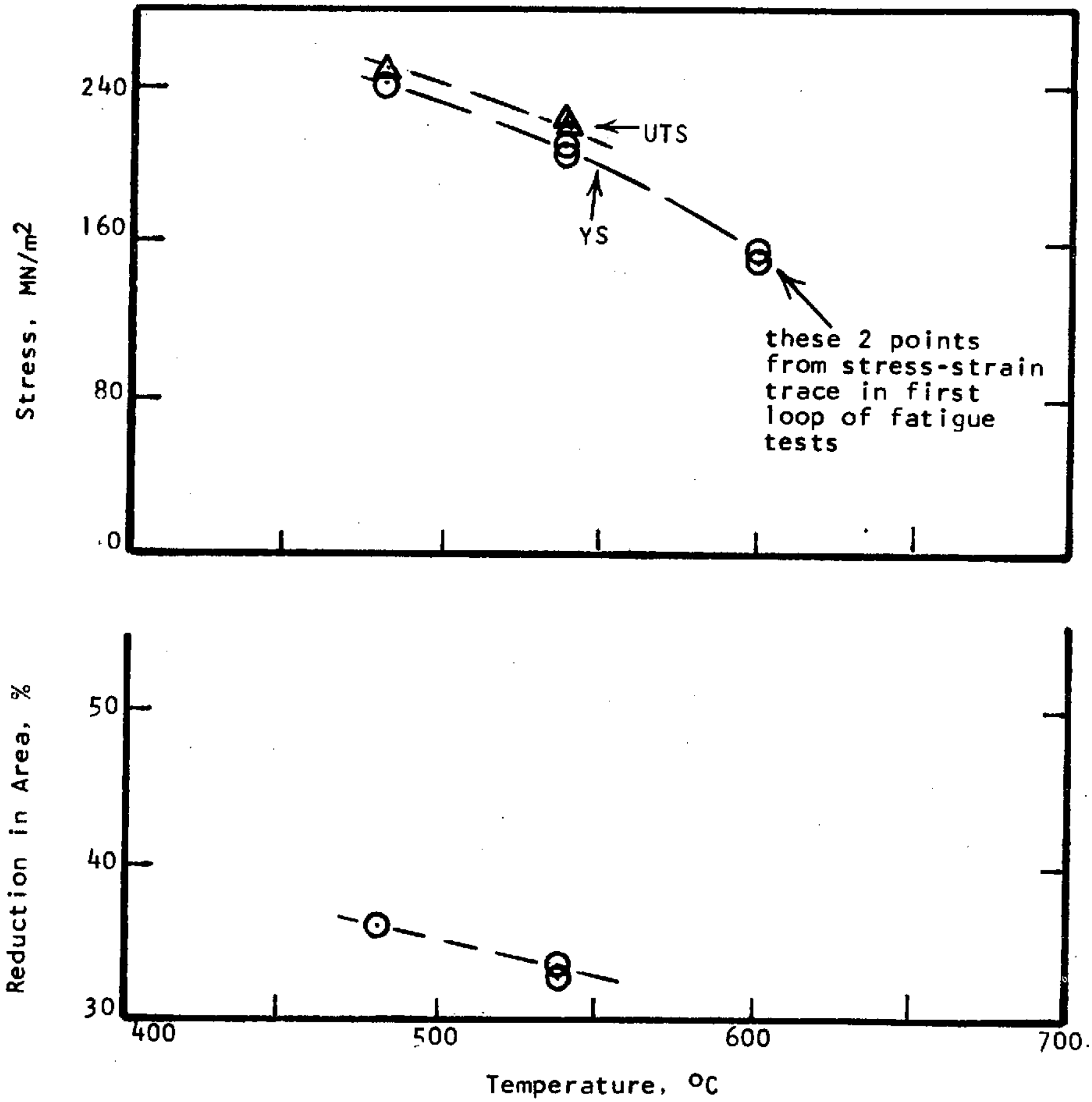

Figure 3 - Tensile properties of R-22 alloy as a function of temperature at a strain rate of 2×10^{-3} sec^{-1}.

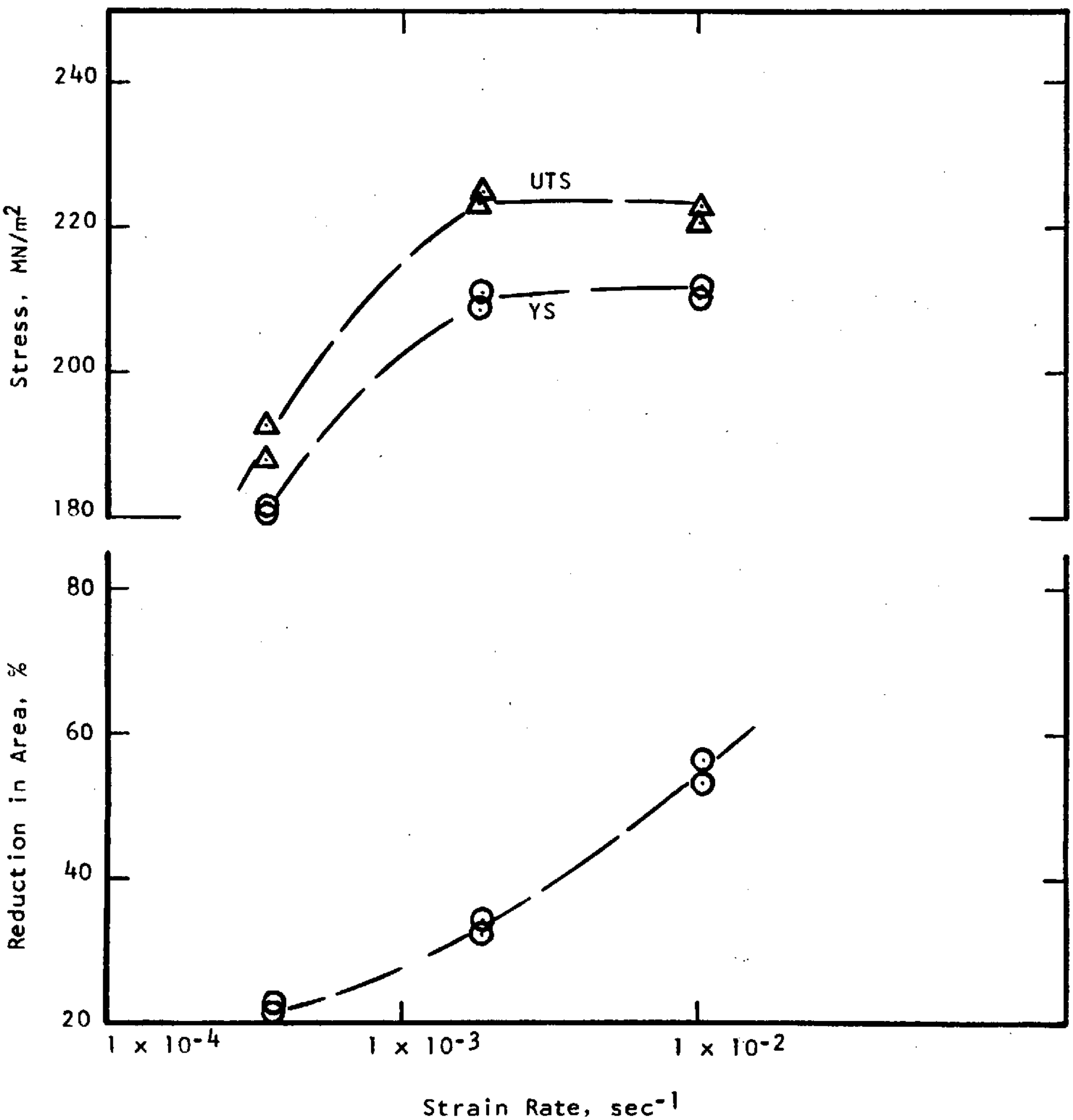

Figure 4 - Tensile Properties of R-22 alloy at 538°C as a function of strain rate.

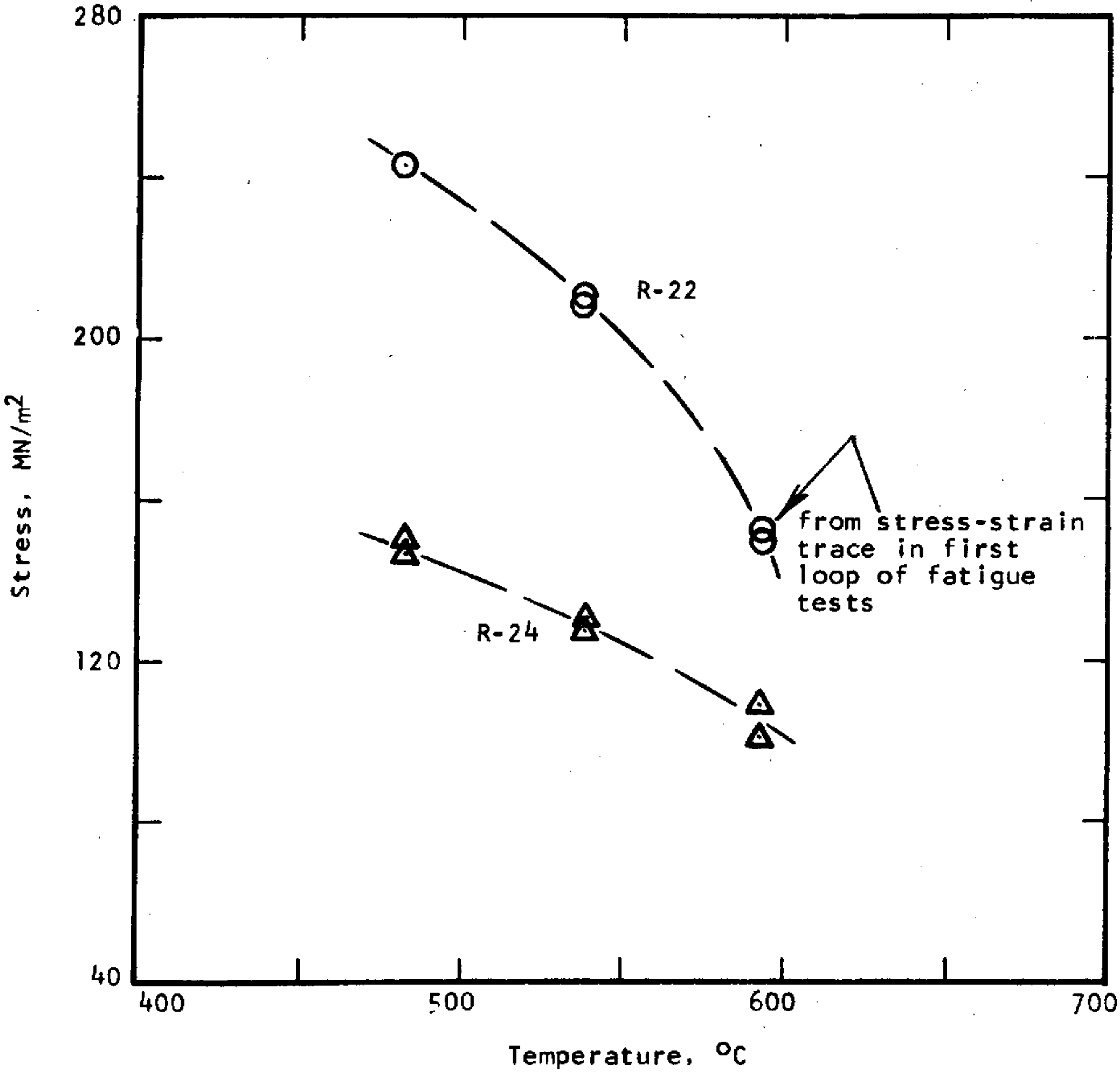

Figure 5 - Comparison of yield strength data for R-22 and R-24 alloys at a strain rate of 2×10^{-3} sec^{-1}.

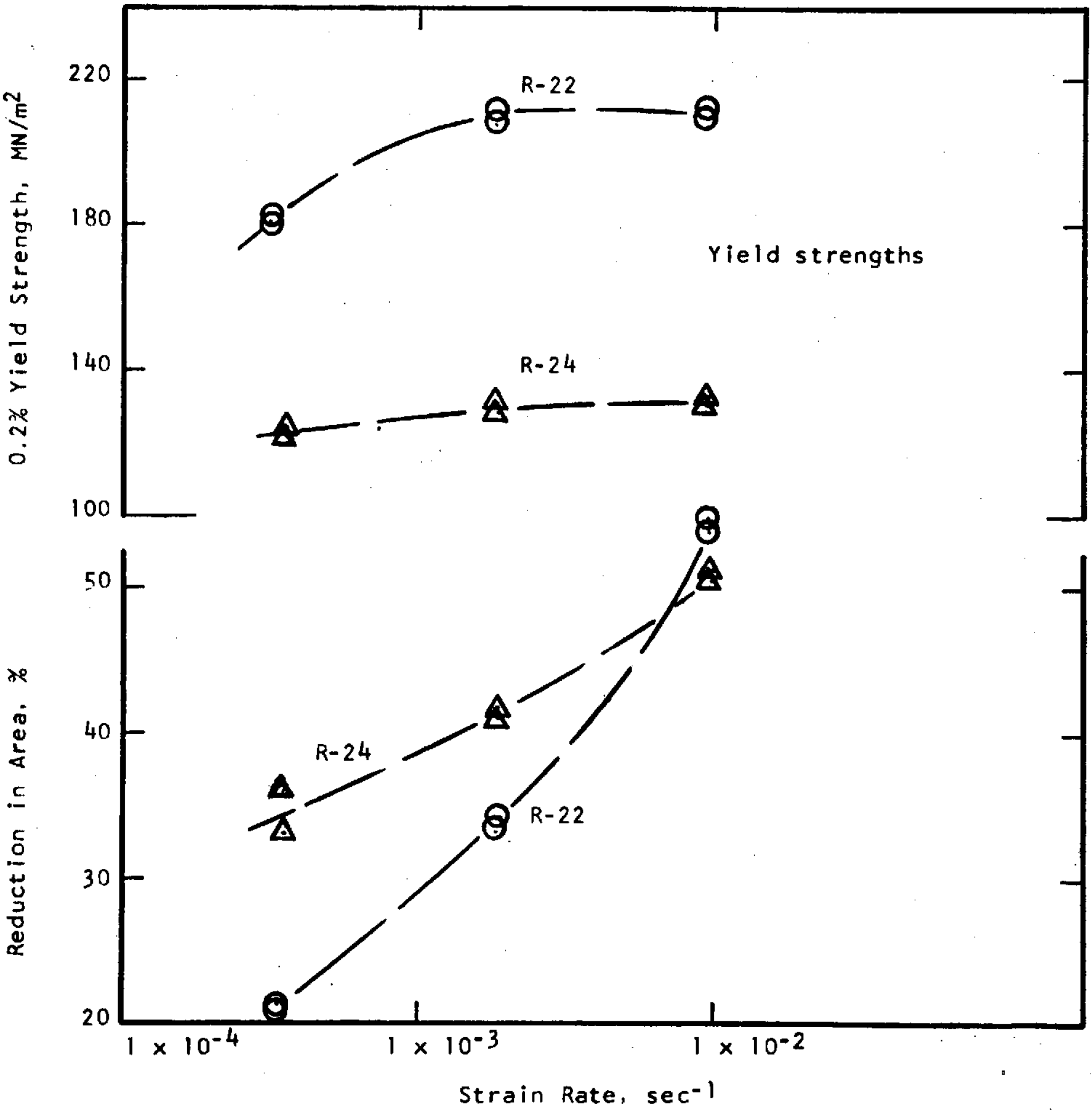

Figure 6 - Comparison of yield strength and reduction in area data for R-22 and R-24 alloys tested at 538°C.

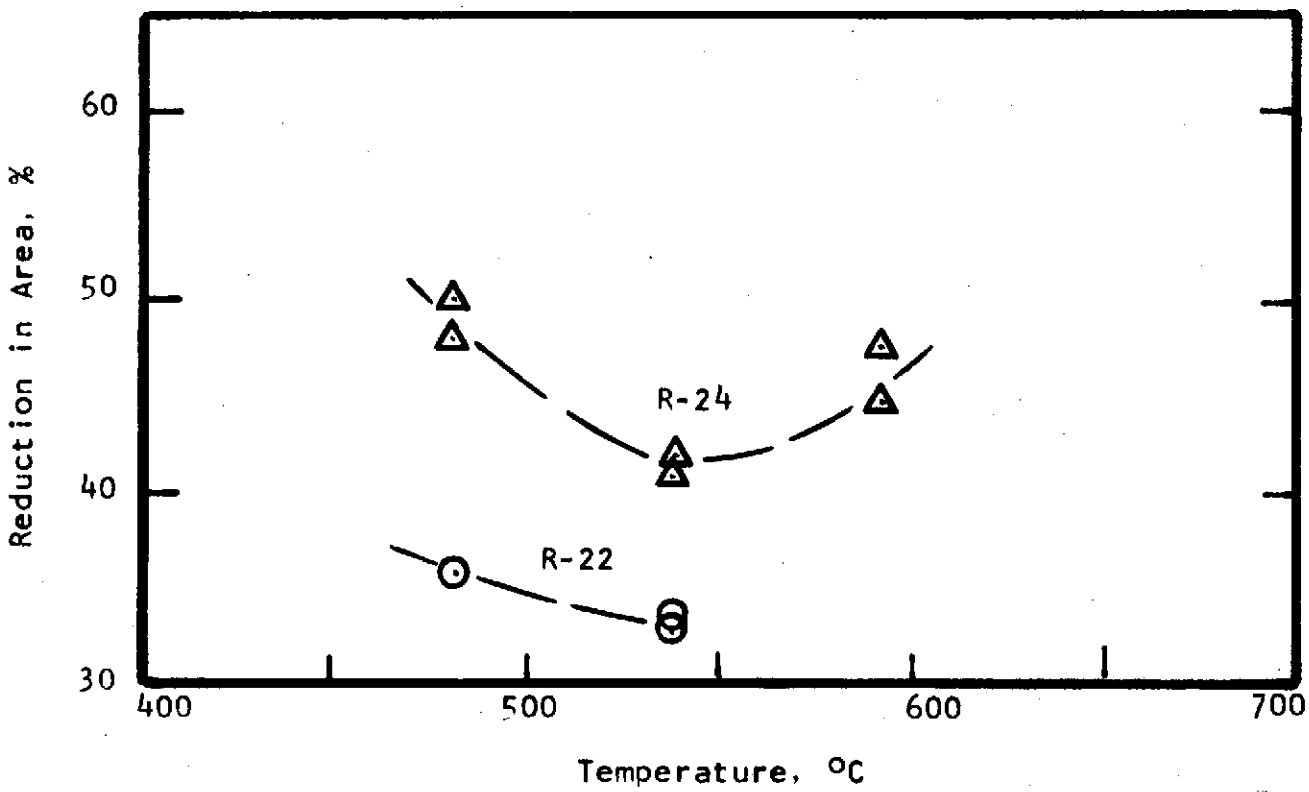

Figure 7 - Comparison of reduction in area values for R-22 and R-24 alloys tested at a strain rate of 2×10^{-3} sec^{-1}.

of the R-22 alloy is much higher than that for the R-24 composition. A similar pattern is noted in the strain rate plot shown in Figure 6. It can be noted, however, that the R-24 composition does exhibit a higher ductility than the R-22 alloy.

A decided strain softening effect was observed in the tensile tests (also noted in the fatigue tests described in a later section of this report) of the R-22 material. The peak force in these tests was observed to occur at very low (about 1%) total strain values and the force trace thereafter indicated a decay rate that was greater than that which could be explained by simply the reduction in area of the specimen. This point is illustrated in Figure 8 which presents true stress versus true strain plots for these R-22 specimens at true axial strain rates of 0.04, 0.2 and 1.0 percent per second. In addition, the reduction in area values are included for comparison purposes. Both the slope of these plots and the final reduction in area values as a function of strain rate indicate that a significant amount of creep is occurring during the tensile test.

B) Low-Cycle Fatigue

1) Continuous Cycling Behavior at 538°C and a Strain Rate of 2×10^{-3} sec^{-1}

Four axial strain controlled low-cycle fatigue tests were performed in an evaluation of the R-21, R-22, R-23 and R-25 compositions (a single test of the R-26 material was also performed). These evaluations were performed in argon and employed a test temperature of 538°C, and a strain rate of 2×10^{-3} sec^{-1} to define the fatigue life over the range from 100 to 3000 cycles. A summary of these test results is presented in Tables 4 through 7. In addition to listing various stress and strain components for each test the number of cycles to failure is given along with a comment relating to whether the material cyclic hardened or softened. For each test some attempt was also made to identify a value for N_5, the number of cycles corresponding to a five percent reduction in load below the stabilized or equilibrium value. This did not prove to be very successful, however, since in many tests a cyclic softening was exhibited and a stabilized load value was never achieved. Furthermore, in a few tests the position of the extensometer tips with respect to the location of the crack actually caused the load to increase slightly as failure approached. Because of these complications the identification of N_5 values was abandoned and some other expression of impending failure was adopted. Each test was evaluated by analyzing the load and plastic strain traces to determine that point within each test at which some change in these recordings would suggest that the crack size had become sufficiently large to indicate that the specimen was beginning to fail. This value was N^* and was expressed as a fraction of N_f, the cycles to failure. While there was about 10 to 15 percent scatter in a

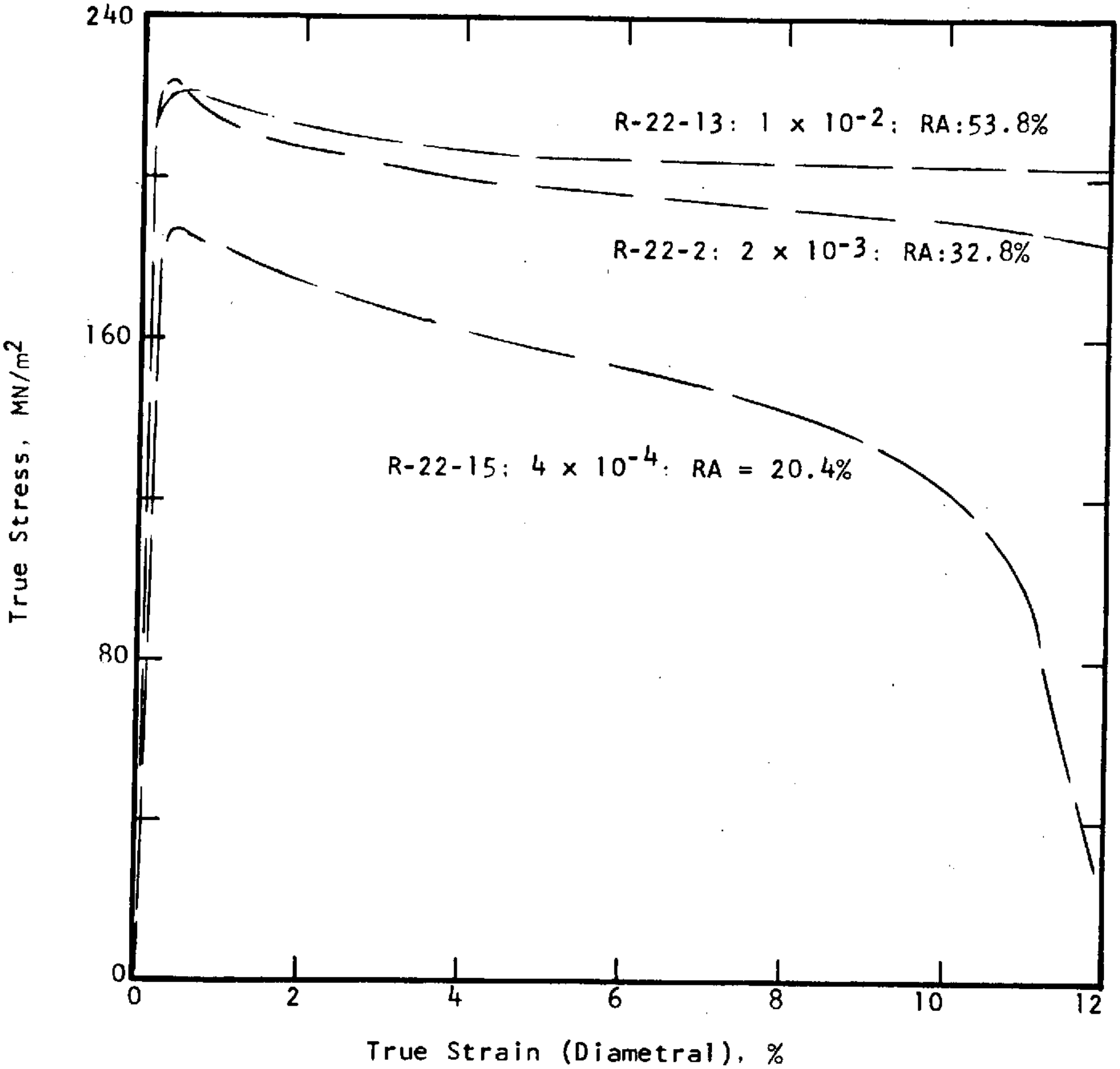

Figure 8 - True stress-strain behavior for R-22 alloy tested at 538°C using various strain rates.

Table 4 - Low-Cycle Fatigue Test Results Obtained in Argon at 538°C Using a Strain Rate of 2×10^{-3} sec^{-1}

R-21 Series
NASA 1-1A alloy,
Aged

Axial Strain Control
A - ratio of infinity
E = 88.9×10^3 MN/m^2

Spec. No.	Poisson's Ratio	Total Strain Range, %	Freq. cpm	Stress Range at Start, MN/m^2	at $N_f/2$			N_f, Cycles to Failure	Remarks
					$\Delta\epsilon_p$ %	$\Delta\epsilon_e$ %	$\Delta\sigma$ MN/m^2		
R-21-3	0.34	1.5	4	158	1.29	0.21	184	1101	
R-21-4	0.35	3.0	2	179.0	2.77	0.23	202.7	270	slight initial hardening
R-21-5	0.35	1.0	6	149.2	0.80	0.20	175.1	4120*	
R-21-6	0.35	5.0	1.2	196.6	4.75	0.25	219.3	92	

*extreme dimensional instability (barrelling)

Table 5 - Low-Cycle Fatigue Test Results Obtained in Argon at 538°C Using a Strain Rate of 2×10^{-3} sec^{-1}

R-22 Series
NASA 1-1B alloy,
As-received

Axial Strain Control
A - ratio of infinity
$E = 88.9 \times 10^3$ MN/m^2

Spec. No.	Poisson's Ratio	Total Strain Range, %	Freq. cpm	Stress Range at Start, MN/m^2	at $N_f/2$			N_f, Cycles to Failure	Remarks
					$\Delta\epsilon_p$ %	$\Delta\epsilon_e$ %	$\Delta\sigma$ MN/m^2		
R-22-4	0.35	2.0	3	421.3	1.75	0.25	217.9	488	↑
R-22-5	0.35	4.0	1.5	426.8	3.72	0.28	251.7	106	Softened
R-22-6	0.35	1.5	4	430.2	1.28	0.22	196.5	1,122	
R-22-7	0.35	1.2	5	430.2	0.98	0.22	193.7	1,992	↓

Table 6 - Low-Cycle Fatigue Test Results Obtained in Argon at 538°C Using a Strain Rate of 2×10^{-3} sec^{-1}

R-23 Series
Glidcop AL-10 alloy

Axial Strain Control
A - ratio of infinity
$E = 88.9 \times 10^3$ MN/m^2

Spec. No.	Poisson's* Ratio	Total Strain Range, %	Freq. cpm	Stress Range at Start, MN/m^2	at $N_f/2$ $\Delta\varepsilon_p$ %	$\Delta\varepsilon_e$ %	$\Delta\sigma$ MN/m^2	N_f, Cycles to Failure	Remarks
R-23-4	0.45	1.0	6	270.3	0.70	0.30	267.5	146	slight initial softening
R-23-7	0.45	0.84	7.14	258.9	0.55	0.29	261.3	501	
R-23-6	0.45	0.7	8.57	253.0	0.41	0.29	259.9	710	slight initial hardening
R-23-5	0.45	0.6	10	239.3	0.32	0.28	249.6	2405	

* These values are higher than would be anticipated and are thought to be in error because the value of E specified for use with this material is probably incorrect.

Table 7- Low-Cycle Fatigue Test Results Obtained in Argon at 538°C Using a Strain Rate of 2×10^{-3} sec^{-1}

R-25 Series Sputtered Zr-Cu, annealed and R-26 Series Sputtered Zr-Cu, As-sputtered

Axial Strain Control
A - ratio of infinity
$E = 88.9 \times 10^3$ MN/m^2

Spec. No.	Poisson's Ratio	Total * Strain Range, %	Freq. cpm	Stress Range at Start, MN/m^2	at $N_f/2$ $\Delta\varepsilon_p$ %	$\Delta\varepsilon_e$ %	$\Delta\sigma$ MN/m^2	N_f, Cycles to Failure	Remarks
R-25-6	0.38	2.0	3	191.3	1.79	0.21	186	58	↑
R-25-7	0.38	2.0	3	194.8	1.80	0.20	182.5	109	softened
R-25-8	0.38	1.0	6	190.3	0.81	0.19	168.9	1261	↓
R-25-9	0.39	0.8	7.5	193.1	0.62	0.18	160.7	2392	
R-26-2	0.43	2.0	3	212.4	1.74	0.26	231.7	109	hardened

* Since this material exhibited a decided anisotropy the total strain range values are probably in error; also because of the anisotropy all specimens fractured off center.

plot of N^*/N_f versus log N_f the trend behavior was essentially linear from 0.7 at 100 cycles to 0.90 at 3000 cycles.

A logarithmic plot of the axial strain range versus cycles to failure, N_f, for all the materials involved is presented in Figure 9 . It will be noted that the fatigue characteristics of the R-21 and R-22 materials at 538°C and a strain rate of 2×10^{-3} sec^{-1} are essentially identical over the strain range regime from 1 to 5 percent. It will also be noted that the fatigue life values for the R-23 composition are significantly lower than those for the R-21 and R-22 materials. Similar data for the R-25 and R-26 compositions fall between that exhibited by the R-23 material and that of the R-21 and R-22 compositions. Also presented in Figure 9 is the fatigue curve for the R-24 (Narloy Z) material as reported in NASA CR-134627. This curve appears to identify fatigue life values which are about 50 percent of those established for the R-21 and R-22 alloys. It is also interesting to note that the fatigue resistance of the R-21 and R-22 alloys is noticeably less than that observed for the R-2 (zirconium-copper 1/2 hard alloy) composition in earlier tests.

2) Strain-Rate Effects at 538°C

A study of the effect of strain rate on the fatigue life of the R-22 composition was performed in argon at 538°C using strain rates of 4×10^{-4} and 1×10^{-2} sec^{-1} (duplicate tests which were planned could not be performed because of the limited material available). A summary of the results obtained in these evaluations is presented in Table 8 and a graphical presentation of this information is included in Figure 10. As strain rate is decreased from 1×10^{-2} to 4×10^{-4} sec^{-1} a noticeable decrease in fatigue life is seen to occur. This indicates that a definite creep effect is present and that it serves to decrease the fatigue life as the strain rate is decreased. The magnitude of this creep effect is almost identical to that observed at these same conditions for the R-24 composition reported in NASA CR-134627.

3) Temperature Effects at a Strain Rate of 2×10^{-3} sec^{-1}

A study of the effect of temperature on the fatigue life of the R-22 alloy was performed in argon using a strain rate of 2×10^{-3} sec^{-1} and yielded the results presented in Table 9 (no test could be performed at 482°C and a strain range of 1.2 percent due to the limited amount of material that was available). As shown in Figure 11 no temperature effect was observed at the high strain range over the range from 482° to 593°C; at the lower strain range a slightly longer fatigue life seemed to be indicated as the temperature was increased to 593°C. This observation is, of course, based on very limited information and should be viewed with some reservation until confirmed by additional tests. This effect, it should be noted, is opposite to that observed in the tests of the R-24 composition (see NASA CR-134627) where a noticeable reduction in the fatigue life was noted at a strain range of 0.9 percent as the temperature was increased from 538° to 593°C.

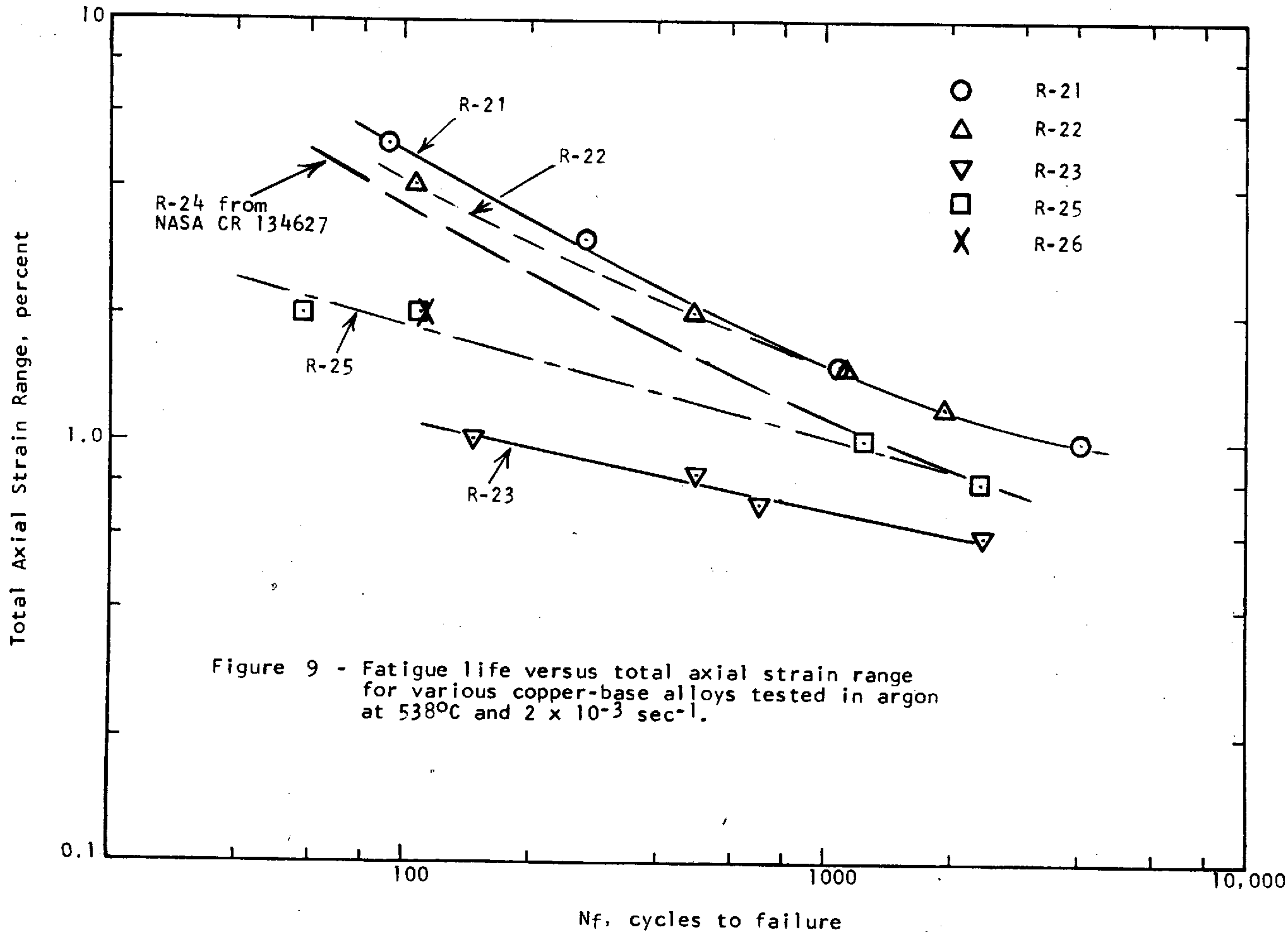

Figure 9 - Fatigue life versus total axial strain range for various copper-base alloys tested in argon at 538°C and 2×10^{-3} sec^{-1}.

Table 8 - Low-Cycle Fatigue Results Obtained in Argon at 538°C Using Strain Rates of 4×10^{-4} and 1×10^{-2} sec $^{-1}$

R-22 Series
NASA 1-1B alloy
As-received

Axial Strain Control
A - Ratio of infinity
E = 88.9×10^3 MN/m2

Spec. No.	Poisson's Ratio	Total Strain Range, %	Freq. cpm	Stress Range at Start, MN/m^2	at $N_f/2$ $\Delta\epsilon_p$ %	$\Delta\epsilon_e$ %	$\Delta\sigma$ MN/m^2	N_f, Cycles to Failure	Remarks
					4×10^{-4} sec $^{-1}$				
R-22-18	0.35	3.0	0.4	372.4	2.79	0.21	182.7	120	Softened
R-22-22	0.35	1.2	1.0	372.4	1.03	0.17	147.5	1224	Softened
					1×10^{-2} sec $^{-1}$				
R-22-19	0.35	3.0	10	470.7	2.66	0.34	301.4	251	Softened
R-22-24	0.35	1.2	25	449.7	0.93	0.27	238.2	2903	Softened

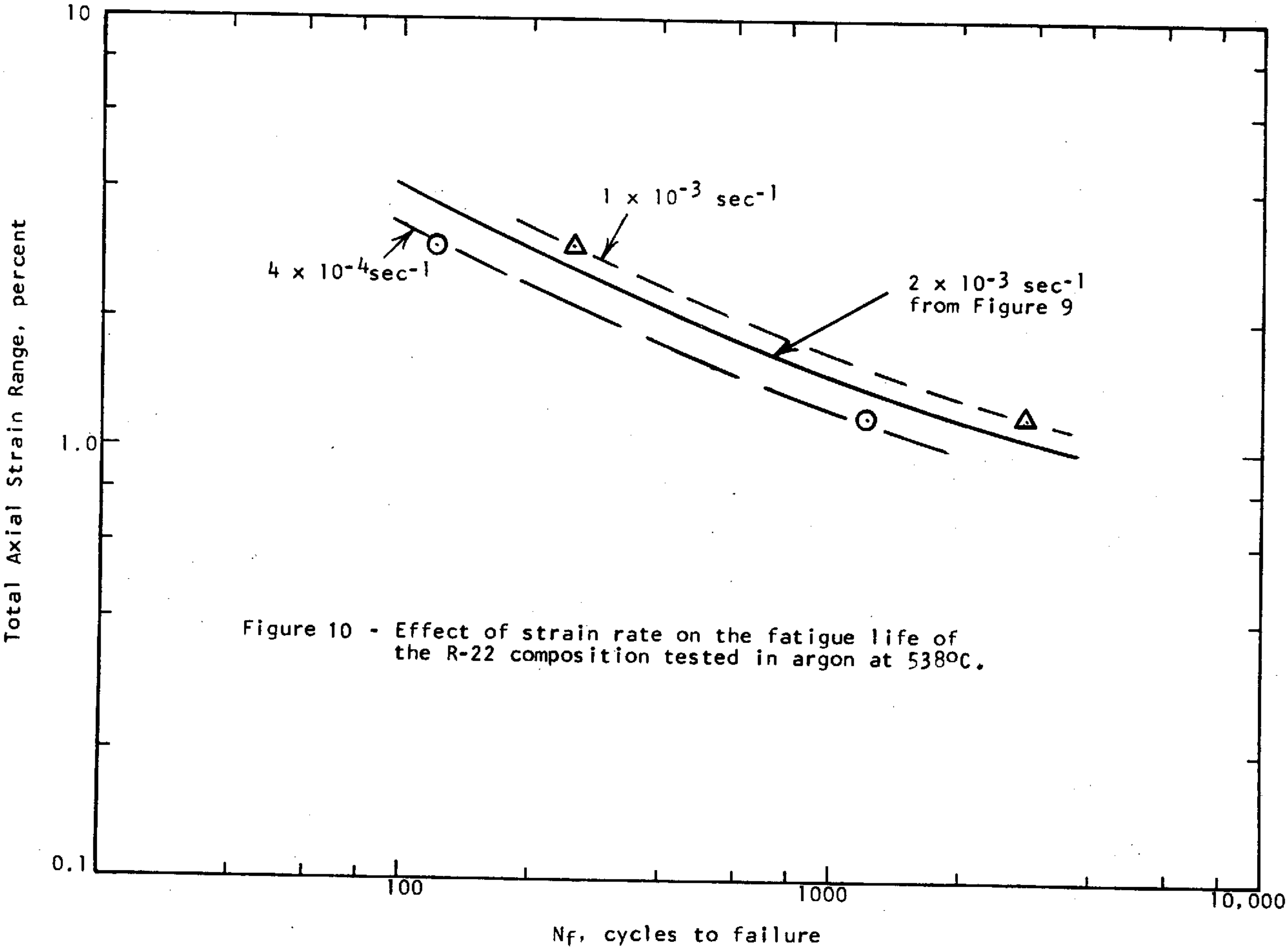

Figure 10 - Effect of strain rate on the fatigue life of the R-22 composition tested in argon at 538°C.

Table 9 - Low-Cycle Fatigue Results Obtained in Argon at 482° and 593°C Using a Strain Rate of 2×10^{-3} sec^{-1}

R-22 Series
NASA 1-1B alloy
As-received

Axial Strain Control
A - ratio of infinity

Spec. No.	Poisson's Ratio	Total Strain Range, %	Freq. cpm	Stress Range at Start, MN/m^2	at $N_f/2$ $\Delta\epsilon_p$ %	$\Delta\epsilon_e$ %	$\Delta\sigma$ MN/m^2	N_f, Cycles to Failure	Remarks
				482°C; $E = 95.8 \times 10^3$ MN/m^2					
R-22-26	0.355	3.0	2.0	512.2	2.64	0.36	347.8	186	Softened
R-22-27	0.355	3.0	2.0	511.5	2.64	0.36	343.6	205	Softened
				593°C; $E = 81.4 \times 10^3$ MN/m^2					
R-22-28	0.35	3.0	2.0	302.1	2.80	0.20	163.7	206	Softened
R-22-29	0.35	3.0	2.0	314.1	2.79	0.21	168.6	192	↓
R-22-33	0.35	1.2	5.0	314.1	1.03	0.17	139.1	2893	↓
R-22-34	0.35	1.2	5.0	313.4	1.02	0.18	143.3	2248	↓

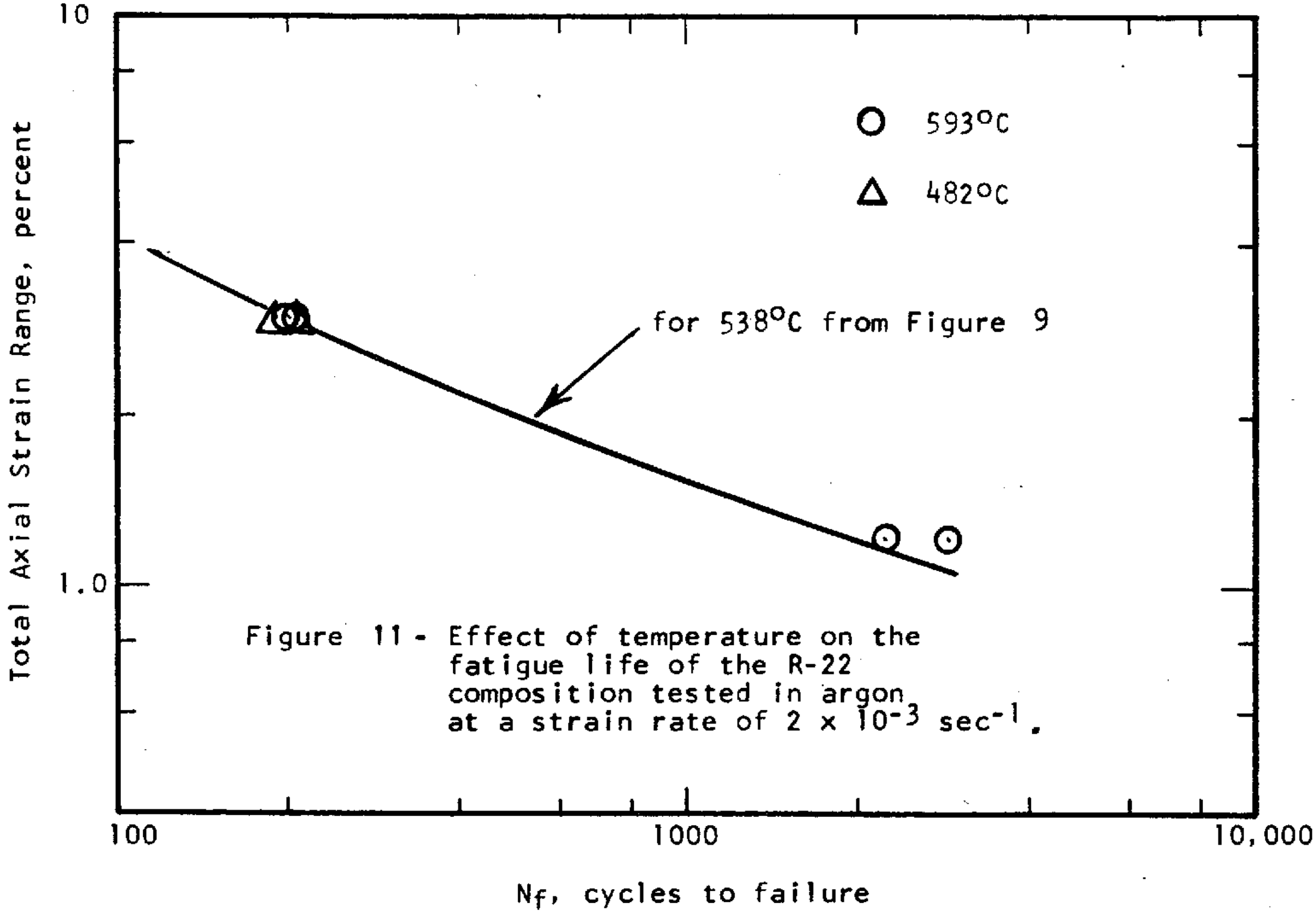

Figure 11 - Effect of temperature on the fatigue life of the R-22 composition tested in argon at a strain rate of 2×10^{-3} sec^{-1}.

4) Hold-Time Effects at 538°C

The effect of a 300-second hold period on the fatigue life of the R-22 alloy was evaluated in argon at 538°C for two different strain ranges. Duplicate tests at the strain range of 3.0 percent were planned but were not performed due to the limited amount of material that was available.

A summary of the test results obtained is presented in Tables 10 and 11 and is seen to include information relating to a hold period in tension only and a hold period in compression only. Some dimensional instability (barrelling) appeared in all tests exceeding 200 cycles and this was particularly pronounced in the compression hold-time tests at a strain-range of 1.2 percent where a very noticeable decrease in specimen length was in evidence as barrelling took place.

A plot of the test results from Table 10 is presented in Figure 12 to reveal an extremely detrimental effect of hold periods in tension at both strain ranges evaluated. The effect is particularly pronounced at the lower strain range where a 300 second hold period is seen to reduce the fatigue life to about 85 cycles from the value of 2000 cycles observed in the continuous cycling tests. This life reduction is much greater than that observed in the tests of the R-24 composition reported in NASA CR-134627.

Hold periods in compression exhibited an effect on the R-22 alloy that depended on strain range. At a strain range of 3.0 percent the compression hold period appeared to lead to a slightly longer fatigue life than that observed in the continuous cycling tests at 538°C. This effect is the same as that reported previously for the R-24 material. In the tests at a strain range of 1.2 percent, however, the fatigue life of the R-22 alloy was found to decrease below the continuous cycling results when a compression hold period was introduced. This result is opposite to that noted for the R-24 composition. Some of this effect might be due to the extreme barrelling which took place in the compression hold time tests of the R-22 alloy at the lower strain range and for this reason some further study of this effect is in order before this behavior pattern can be accepted as completely reliable.

5) Cyclic Strain Hardening and Softening Behavior

While the cyclic stress-strain behavior for all the materials tested is indicated in the data summaries of Tables 4 through 11, several important observations deserve special emphasis. One relates to the different behavior exhibited by the R-21 and R-22 alloys. A cyclic strain hardening was exhibited by the R-21 material at 538°C and as indicated in Table 4 the stress range increased about 10 percent in going from the

Table 10 - Low-Cycle Fatigue Results Obtained in Hold-Time Tests in Argon at 538°C Using a Ramp Strain Rate of 2×10^{-3} sec^{-1}

R-22 Series
NASA 1-1B alloy
As-received

Axial Strain Control
A - ratio of infinity
$E = 88.9 \times 10^3$ MN/m^2

Spec. No.	Poisson's Ratio	Total Strain Range, %	Cycling Data: Ramp Time, sec.	Cycling Data: Hold Time, sec.	N_f, cycles to failure	Remarks
R-22-39	0.35	1.2	12	300 Tension	88	cyclic softened
R-22-40	0.35	1.2	12	300 Tension	81	
R-22-41	0.35	3.0	30	300 Tension	33	
R-22-44	0.35	1.2	12	300 Compression	389	barrelled
R-22-8	0.35	1.2	12	300 Compression	622	barrelled
R-22-42	0.35	3.0	30	300 Compression	282	barrelled

Table 11 - Low-Cycle Fatigue Results Obtained in Hold-Time Tests in Argon at 538°C Using a Ramp Strain Rate of 2×10^{-3} sec^{-1}

R-22 Series
NASA 1-1B alloy
As-received

Axial Strain Control
A - ratio of infinity
$E = 88.9 \times 10^3$ MN/m^2

Spec. No.	Stress Range at Start, MN/m^2	at $N_f/2$						
		$\Delta\sigma$ MN/m^2	σ_t MN/m^2	σ_c MN/m^2	σ_r * MN/m^2	R_σ, Amount of Stress Relaxation MN/m^2	$\Delta\varepsilon_p$ ** %	$\Delta\varepsilon_e$ ** %
R-22-39	404.7	211.5	99.8	111.7	T 21.1	78.7	1.05	0.15
R-22-40	407.5	210.8	104.7	106.1	T 24.6	80.1	1.05	0.15
R-22-41	420.2	253.6	119.4	134.2	T 38.6	80.8	2.81	0.19
R-22-44	428.1	193.0	94.7	98.3	C 31.6	66.7	1.06	0.14
R-22-8	428.1	198.6	98.3	100.3	C 35.1	65.2	1.05	0.15
R-22-42	435.6	212.2	98.4	113.8	C 35.1	78.7	2.85	0.15

*T for tension and C for compression; **based on relaxed stress range

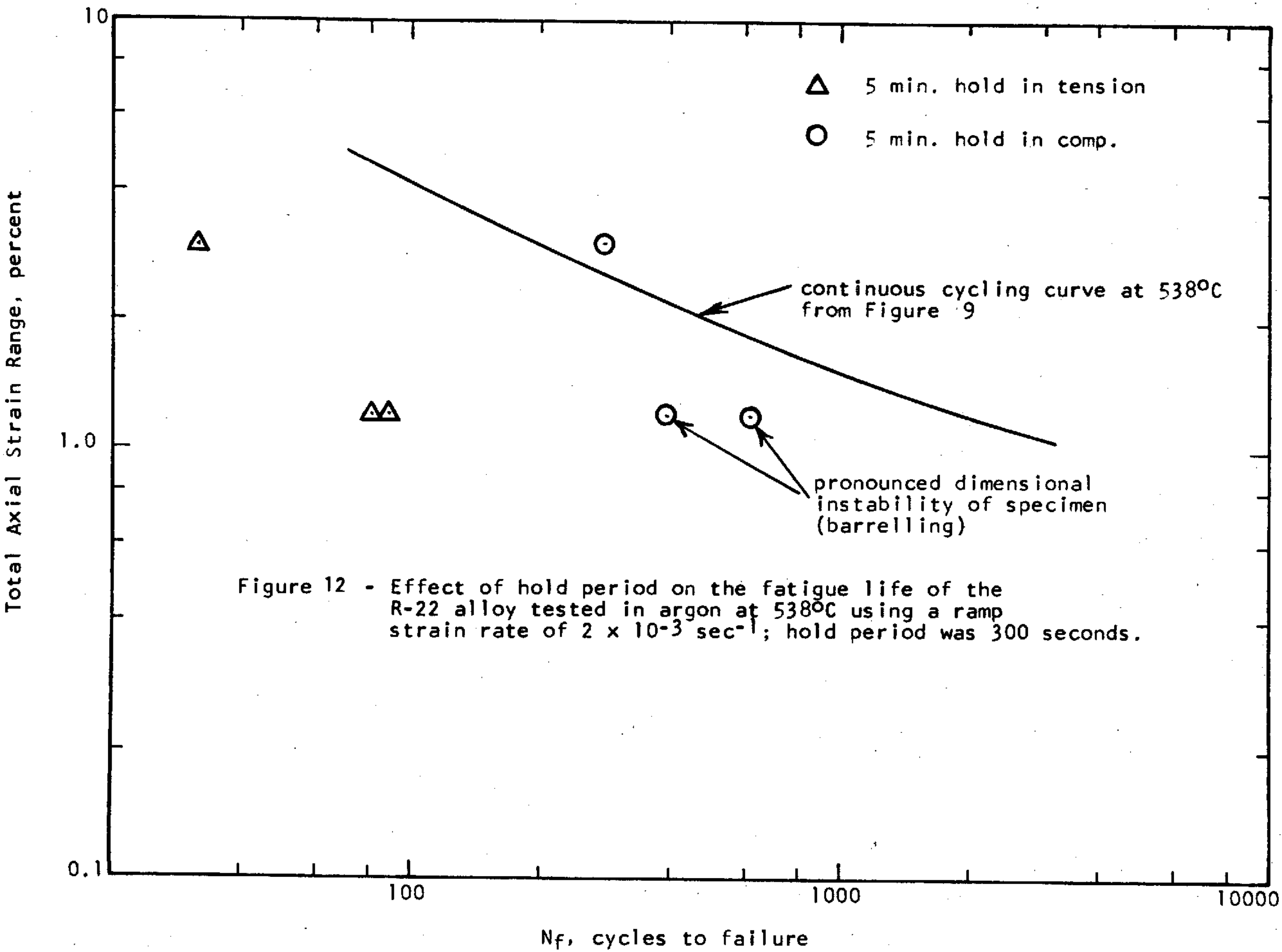

Figure 12 - Effect of hold period on the fatigue life of the R-22 alloy tested in argon at 538°C using a ramp strain rate of 2 x 10^{-3} sec^{-1}; hold period was 300 seconds.

first cycle to $N_f/2$. An inspection of the continuous records of stress range for these tests indicated that most of this increase occurred very early in the test (i.e. up to 0.1 N_f). In the R-22 tests a different cyclic stress-strain response was indicated inasmuch as a very decided cyclic softening was observed. As shown in Table 5 the stress range at $N_f/2$ was about 50 percent of the first cycle value. As with R-21 most of this change in the stress range value occurred within the first 10 percent of the test. It is important to note in these observations that the hardening and softening response is in complete accord with the ratio of σ_{ult}/σ_{ys} as described by Smith, Hirschberg and Manson (NASA-TN-D-1574, 1963). When this ratio is 1.4 or greater a cyclic strain hardening should be exhibited whereas a cyclic strain softening should be exhibited when this ratio is below 1.2. The tensile data in Table 2 indicate that this ratio for R-21 is greater than 1.4 while it is less than 1.2 for the R-22 material.

A comparison of the cyclic stress-strain behavior for the R-22 and R-24 (reported in NASA CR-134627) alloys as measured at $N_f/2$ for 538°C and a strain rate of 2×10^{-3} sec^{-1} is presented in Figure 13. Over the strain ranges studied the stress range for the R-24 alloy is some 20 percent greater than that for the R-22 material.

6) Relaxation Behavior

For each hold-time test the continuous load-time record provided a relaxation curve for each hold period. A typical cycle near half-life was selected from each hold-time test and load-time combinations were chosen at various intervals throughout the hold period to define the relaxation curves presented in Figures 14 through 19. These curves along with the R_σ data in Table 11 enable some comparison to be made of the relaxation behavior exhibited in the several different tests performed in this program. Actually no large differences in relaxation characteristics are in evidence and the difference between tension and compression relaxation appears slight. A plot of $(\sigma_o - \sigma)/\sigma_o$ versus time has been prepared and is shown in Figure 20. These results illustrate the very similar relaxation behavior noted in all these tests(σ_o is the stress value at the start of the hold period).

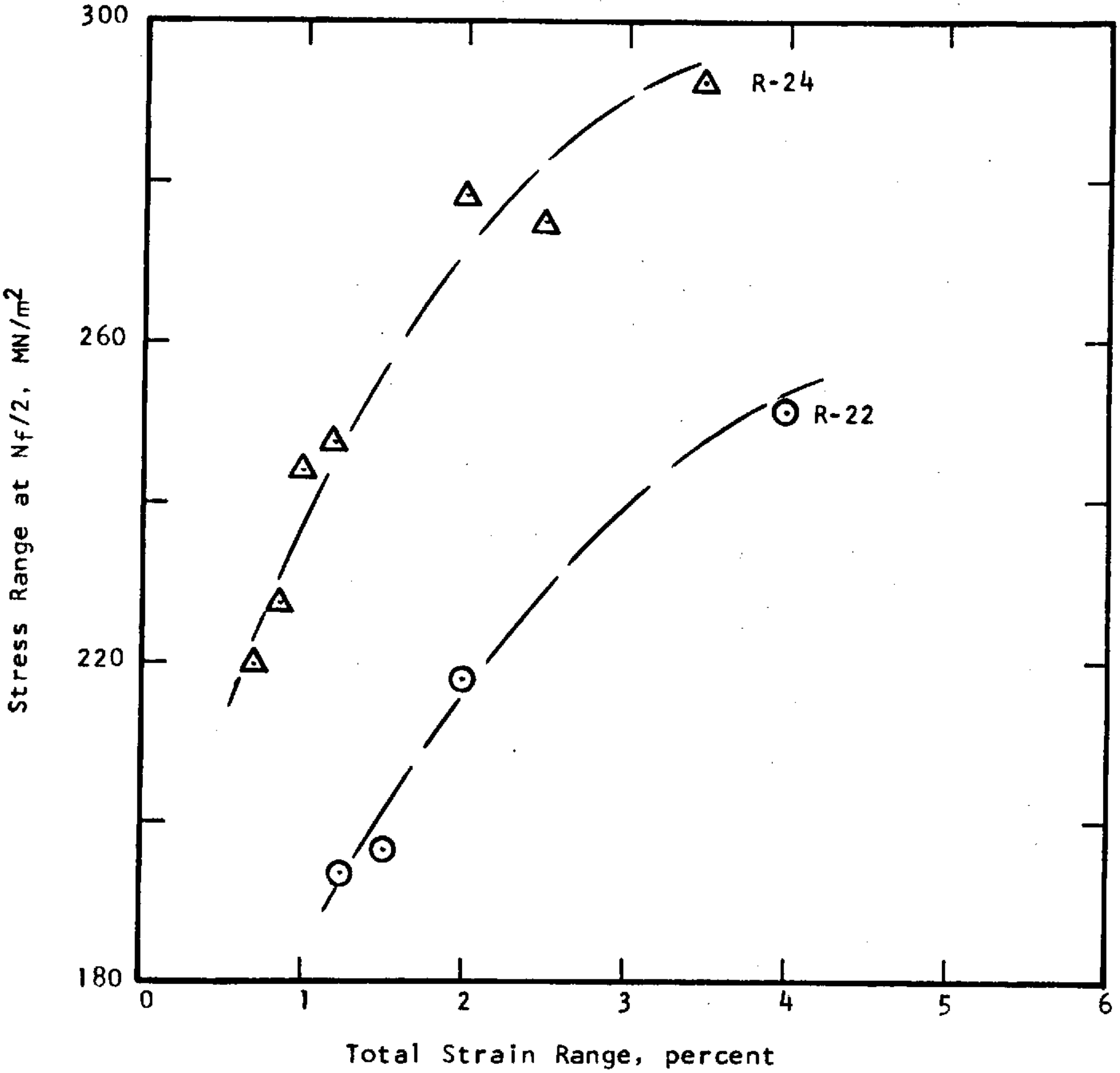

Figure 13 - Comparison of cyclic stress-strain behavior of R-22 and R-24 alloys at $N_f/2$, 538°C and a strain rate of 2×10^{-3} sec^{-1}.

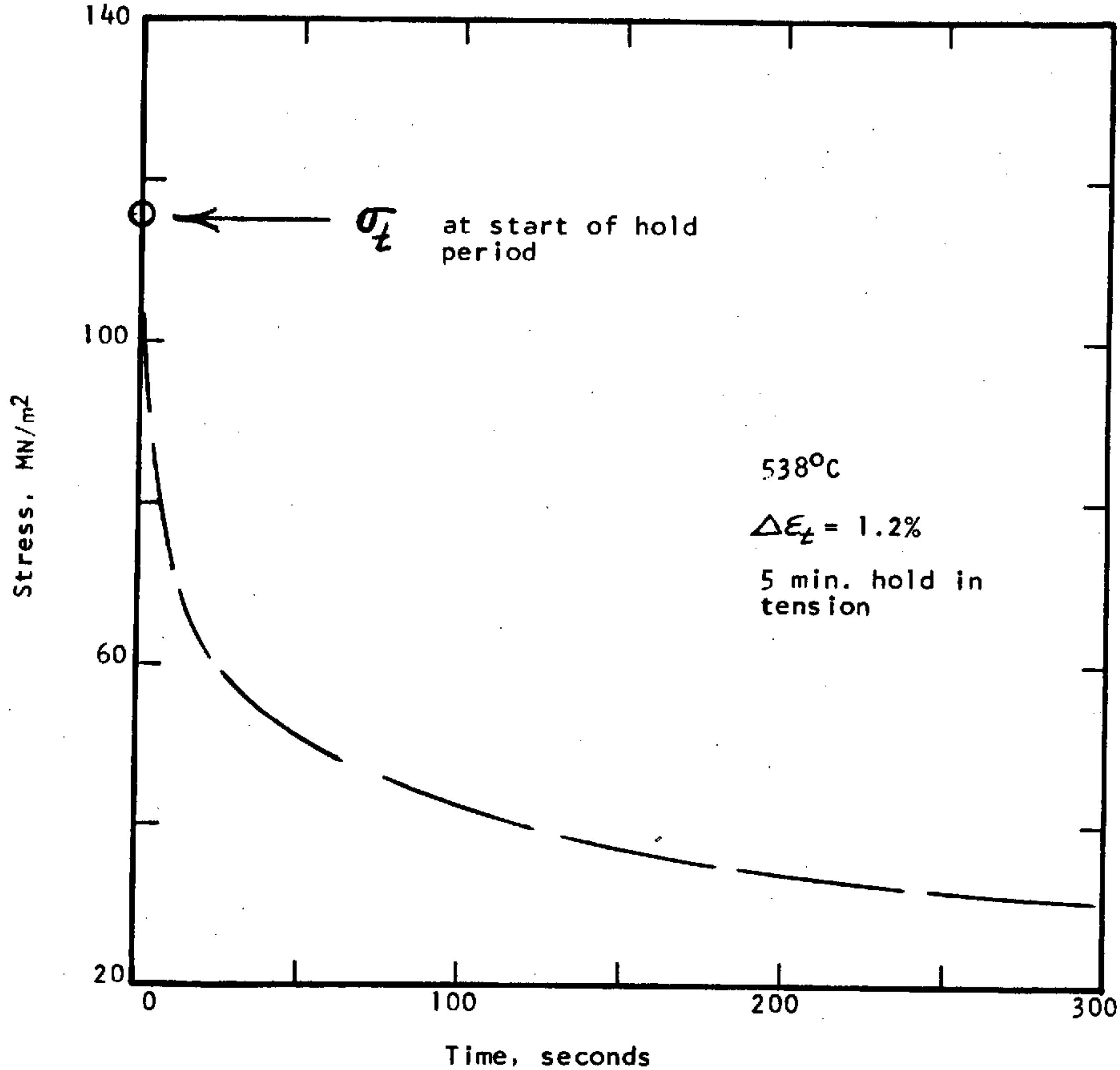

Figure 14 - Relaxation curve near half-life for specimen R-22-39

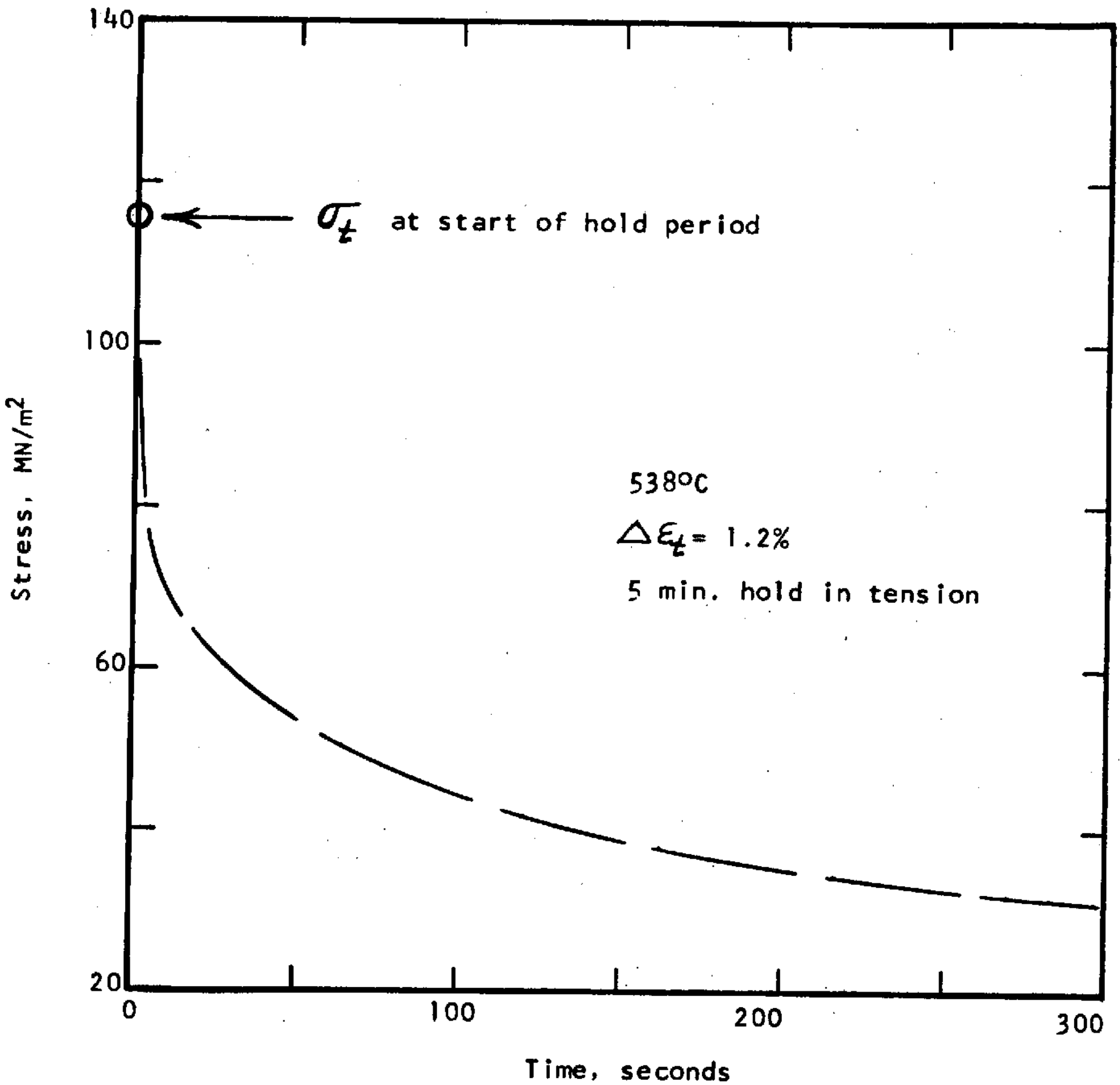

Figure 15 - Relaxation curve near half-life for Specimen R-22-40

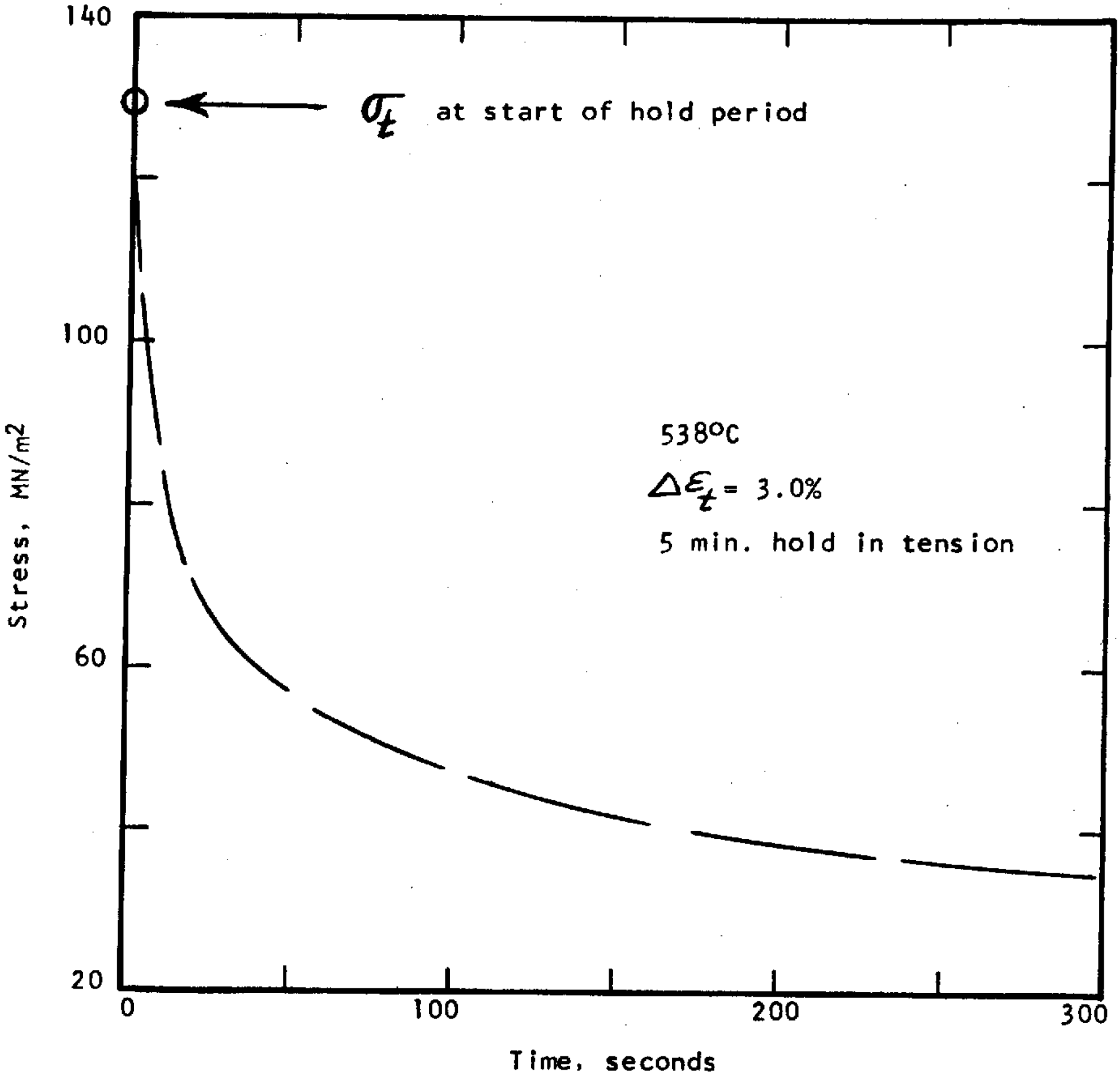

Figure 16 - Relaxation curve near half-life for Specimen R-22-41

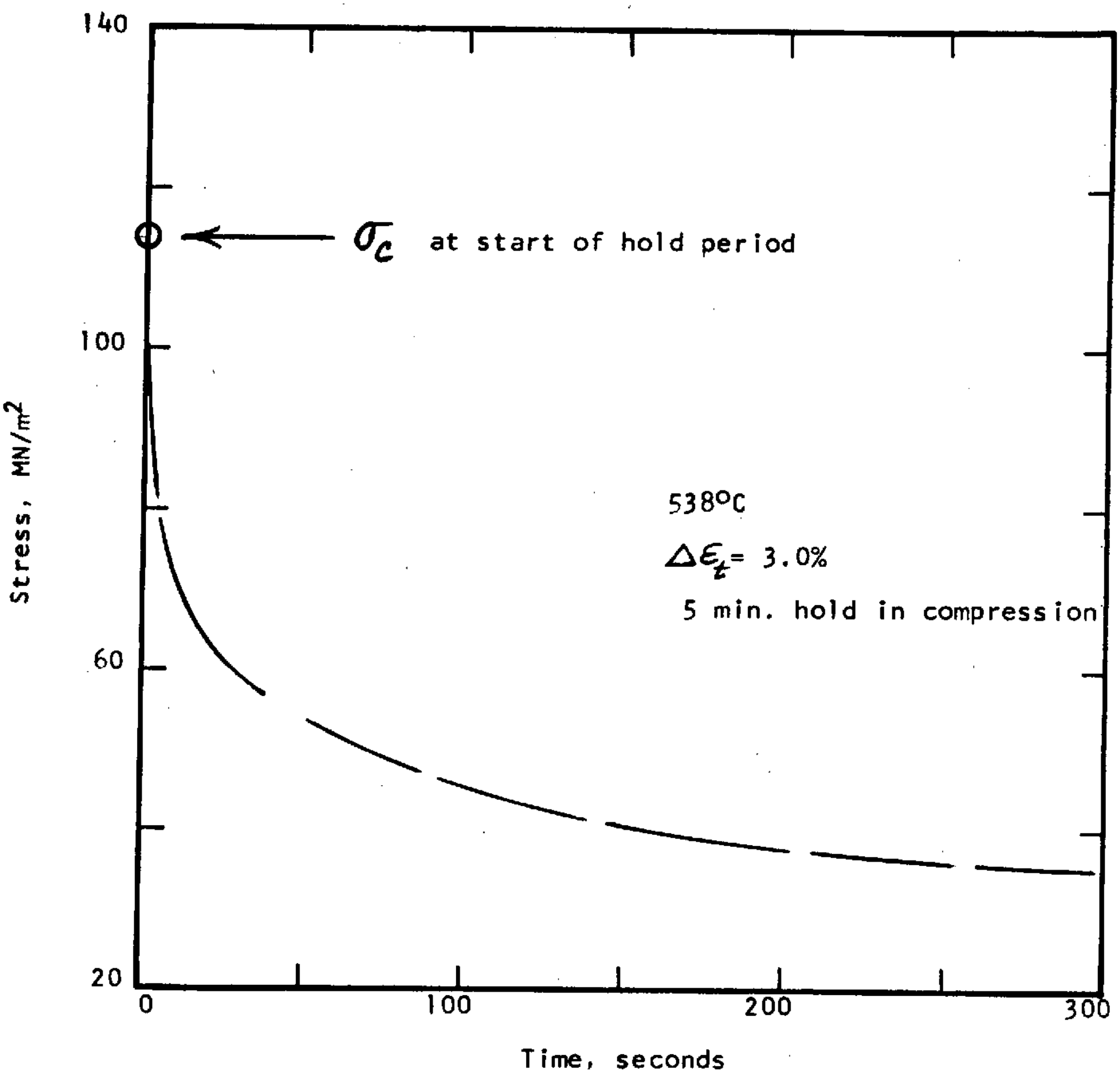

Figure 17 - Relaxation curve near half-life for Specimen R-22-42

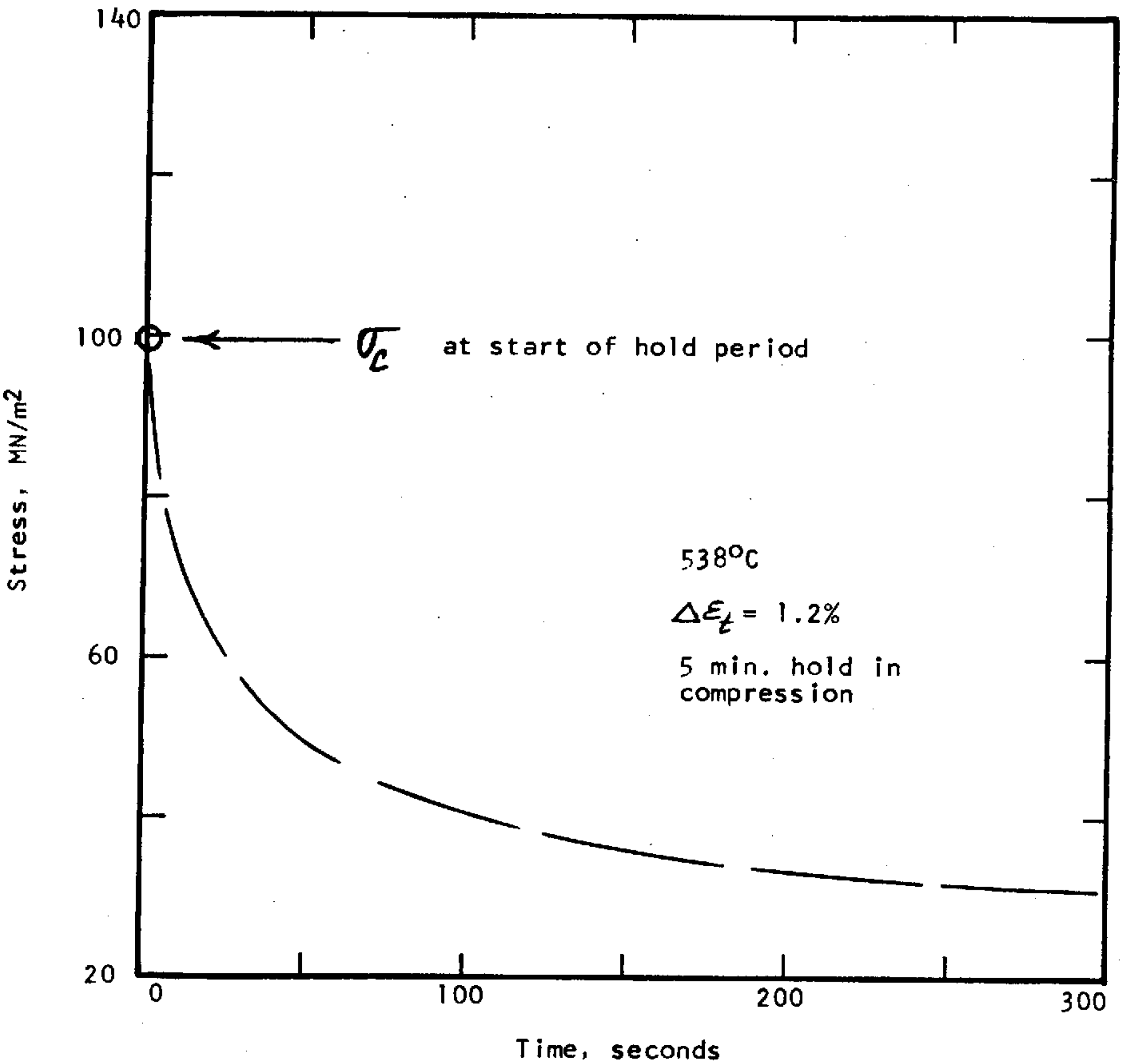

Figure 18 - Relaxation curve near half-life for Specimen R-22-44

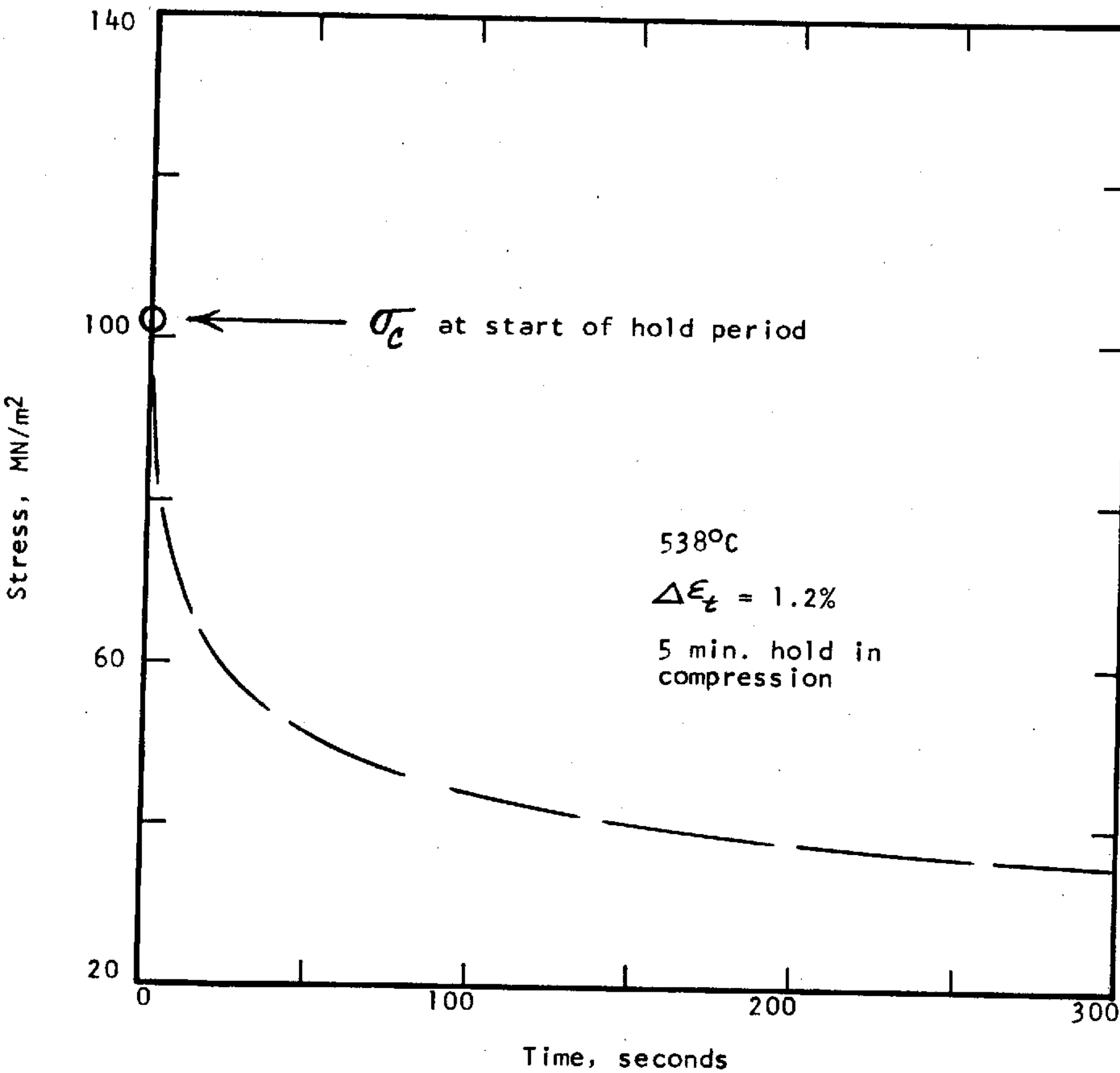

Figure 19 - Relaxation curve near half-life for Specimen R-22-8

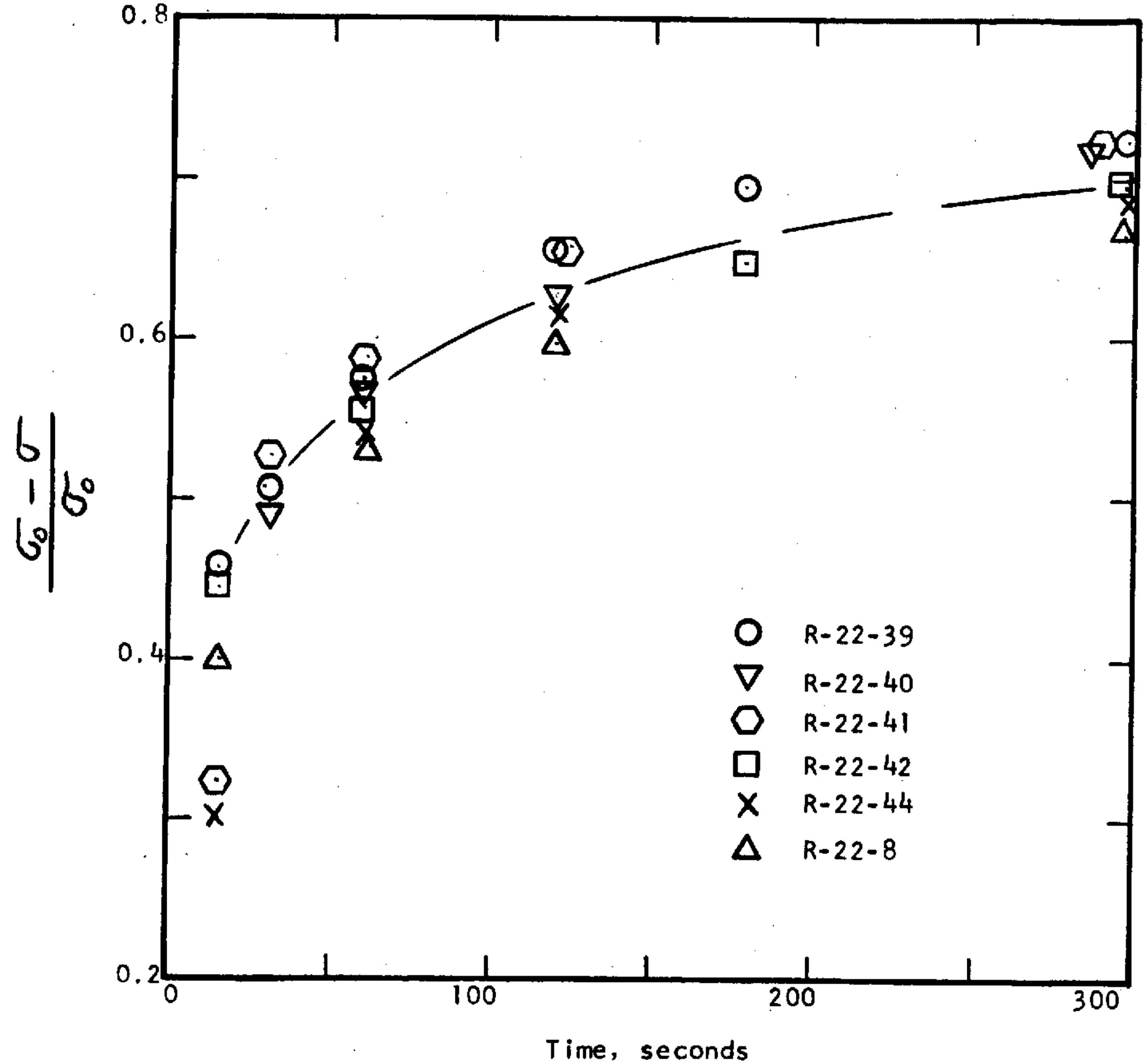

Figure 20 - Comparison of relaxation data for R-22 material.

V - CONCLUSIONS

This report presents a discussion of the test results obtained in an evaluation of the short-term tensile and low-cycle fatigue behavior of five copper-base alloys: NASAl-1A, NASAl-1B Glidcop AL-10, sputtered Zr-Cu (as - received) and sputtered Zr-Cu (annealed). All tests were performed in high purity argon and involved the temperature range from 482° to 593°C and the strain rate regime from 4×10^{-4} to 1×10^{-2} sec^{-1}.

Short-term tensile data were reported for all five materials tested in argon at 538°C using a strain rate of 2×10^{-3} sec^{-1}. The yield and tensile strengths of the R-22 material were essentially twice those of the R-21, R-25 and R-26 materials and somewhat less than twice those of the R-23 compositions. Ultimate tensile strengths ranged from a high of about 220 MN/m^2 for R-22 to a low of 84.7 MN/m^2 for the R-26 material. Ductilities (reduction in areas) ranged from about 98 percent for the R-25 and R-26 materials to 33 percent for R-22, 50 to 55 percent for R-21, to 5 to 7 percent for R-23.

Short-term tensile data for the R-22 material are reported as a function of strain rate at 538°C and as a function of temperature at a strain rate of 2×10^{-3} sec^{-1}. As the strain rate is increased from 4×10^{-4} to 1×10^{-2} sec^{-1} at 538° C the yield strength, ultimate tensile strength and reduction in area values exhibited definite increases. Reduction in area values are seen to increase by more than a factor of two over this strain rate regime. Temperature effects at a strain rate of 2×10^{-3} sec^{-1} were also noticeable over the range of 482° to 593°C. The biggest effect is a decrease in yield strength from about 220 MN/m^2 to about 150 MN/m^2 as the temperature was increased from 538° to 593°C. The yield and ultimate tensile strengths of the R-22 alloy are much greater than those of the R-24 (Narloy Z) composition at the temperature studied in the program with the strength differential reaching 50 percent at 538°C and above. In terms of reduction in area, however, the values for the R-24 material are noticeably higher than those for the R-22 material except in the higher strain rate regime at 538°C where the values are essentially the same.

Axial strain controlled low-cycle fatigue tests in argon at 538°C and a strain rate of 2×10^{-3} sec^{-1} indicated essentially identical behavior for the R-21 and R-22 compositions. The R-23 composition exhibited the lowest fatigue resistance of all the materials tested while the fatigue behavior of the R-25 and R-26 compositions appeared to be between the lower limit defined by R-26 and the upper limit defined by the R-21 and R-22 data. At this temperature and strain rate the fatigue life defined for R-21 and R-22 is about twice that reported previously for the R-24 composition.

Strain rate effects on the low-cycle fatigue life of the R-22 alloy tested in argon at 538°C were noticeable and led to a reduction in N_f as the strain rate was decreased from 1×10^{-2} to 4×10^{-4} sec^{-1}. At a strain rate of 2×10^{-3} sec^{-1} the effect of temperature on the fatigue life of R-22 was negligible at a strain range of 3.0 percent as the temperature was increased from 482° to 593°C. At a strain range of 1.2 percent some slight increase in fatigue life was indicated as the temperature was increased from 538° to 593°C.

Hold period durations of 300 seconds were employed at 538°C and a strain rate of 2×10^{-3} sec^{-1} in an evaluation of the low-cycle fatigue behavior of R-22 using two different strain ranges. Hold periods in tension were much more detrimental than hold periods in compression in that the fatigue life was reduced much below that for continuous cycling. The effect ranged from just below an order of magnitude at a strain range of 3.0 percent to much more than an order of magnitude at a strain range of 1.2 percent. Hold periods in compression, on the other hand, led to two different behavior patterns. At a strain range of 3.0 percent the effect was close to being negligible whereas at a strain range of 1.2 percent the fatigue life was reduced from about 2000 cycles in continuous cycling to about 500 cycles with the compression hold period. The tests involving the compression hold periods exhibited severe barrelling so that these conclusions must be viewed with some qualification.

Relaxation data obtained in the hold-time tests are compared. It is shown that the tension and compression relaxation characteristics are quite similar.

Distribution List for this Report

Carlen, Prof A E
Box 2908
AME Dept
University, AL 35486

Coffin, Dr L F Jr
G E - Corp R&D Lab
Box 8
Schenectady, NY 12301

Cooper, R R
Rocketdyne AC14
6633 Canoga Ave
Canoga Park, CA 91304

Harrod, D L
Westinghouse
Rm 2A31 Bldg 401
1310 Beulah Rd
Pittsburgh, PA 15235

Jaske, C E
BMI
505 King Ave
Columbus, OH 43201

Lee, F F
22421 Philiprimm St
Woodland Hills, CA 91364

Morrow, Prof J
321 Talbot Lab
Univ of Ill
Urbana, IL 61801

Sheffler, Dr K D
P&W Aircraft
MERL, Bldg 140
Middletown, CT 06457

Van Wanderham, M B08
P&W Aircraft
W Palm Beach, FL 33402

Wundt, B M
2346 Shirl Lane
Schenectady, NY 12309

NASA Rep (10)
Sci & Tech Info Facility
Box 33
College Park, MD 20740

Defense Documentation Ctr
Cameron Station
5010 Duke St
Alexandria, VA 22314

MCIC
Battelle Memorial Inst
505 King Ave
Columbus, OH 43201

Tech Reports Library (3)
U S AEC
Washington, DC

Tech Info Service (3)
U S AEC
Box 62
Oak Ridge, TN

Project Manager (6)
NASA-Lewis
21000 Brookpark Rd
Cleveland, OH 44135

Library
NASA
Langley Research Ctr
Langley Field, VA 23365

Library
NASA
Marshall Space Flight Ctr
Huntsville, AL 35812

Gregory, J W
MS 500-203
NASA-Lewis Research Ctr
21000 Brookpark Rd
Cleveland, OH 44135

Tomazic, W A
MS 500-203
NASA-Lewis Research Ctr
21000 Brookpark Rd
Cleveland, OH 44135

Aukerman, C A
MS 500-204
NASA-Lewis Research Ctr
21000 Brookpark Rd
Cleveland, OH 44135

Powell, W
NASA-Pasadena Office
4800 Oak Grove Dr
Pasadena, CA 91103

Schlemmer, N
Bldg 4610
NASA-Marshall
Huntsville, AL 35812

McPherson, W B
Bldg 4612
S&E - ASTN - MMM
NASA-Marshall
Huntsville, AL 35812

Jamison, R
Brush-Wellman
17876 St Claire Ave
Cleveland, OH 44110

Barrett, E T/M 3417
TRW
23555 Euclid Ave
Cleveland, OH 44117

Buckman, R W Jr
Westinghouse - ANL
Box 10864
Pittsburgh, PA 91304

Somerville, J
Rockwell Intnl
Rocketdyne Div
6633 Canoga Ave
Canoga Park, CA 91304

Elliot, J
Rockwell Intnl
Rocketdyne Div
6633 Canoga Ave
Canoga Park, CA 91304

Sims, J
Bldg 2001, Dept 2202
Aerojet
Box 13222
Sacremento, CA 95813

Kehl, W
Amax Copper, Inc
1270 Ave of the Americas
New York, NY 10020

Marchitto, M F
Glidden-Durkee
Metals Group
900 Union Commerce Bldg
Cleveland, OH 44115

Tech Library / JM6
NASA
Manned Spacecraft Ctr
Houston, TX 77058

Library - Acquisitions
NASA - JPL
4800 Oak Grove Dr
Pasadena, CA 91102

Library
NASA
Goddard Space Flight Ctr
Greenbelt, MD 20771

Library
NASA
Flight Research Ctr
P O Box 273
Edwards, CA 93523

Library MS 202-3
NASA
Ames Research Ctr
Moffett Field, CA 94035

Deutsch, G C /RW
NASA Headquarters
Washington, DC 20546

Harris, Dr L A /RUS
NASA Headquarters
Washington, DC 20546

Technology Utilization
NASA MS 3-19
Lewis Research Ctr
21000 Brookpark Rd
Cleveland, OH 44135

Report Control Office
NASA MS 5-5
Lewis Research Ctr
21000 Brookpark Rd
Cleveland, OH 44135

Patent Council
NASA MS 500-311
Lewis Research Ctr
21000 Brookpark Rd
Cleveland, OH 44135

Library (2)
NASA MS 60-3
Lewis Research Ctr
21000 Brookpark Rd
Cleveland, OH 44135

Contracts Sect B
NASA MS 500-313
Lewis Research Ctr
21000 Brookpark Rd
Cleveland, OH 44135

Ault, G M
MS 3-5
NASA-Lewis Research Ctr
21000 Brookpark Rd
Cleveland, OH 44135

Assoc Chief, M&S Div
MS 49-1
NASA-Lewis Research Ctr
21000 Brookpark Rd
Cleveland, OH 44135

Chief, M&S Div 49-1
Report File
NASA-Lewis Research Ctr
21000 Brookpark Rd
Cleveland, OH 44135

Head, Fatigue Res Sect
MS 49-1
NASA-Lewis Research Ctr
21000 Brookpark Rd
Cleveland, OH 44135

Kazaroff, J M (7)
MS 500-209
NASA-Lewis Research Ctr
21000 Brookpark Rd
Cleveland, OH 44135

Herr, P /RS
NASA Headquarters
Washington, DC 20546